Lithos 150 (2012) 49–61

Contents lists available at SciVerse ScienceDirect

Lithos

journal homepage: www.elsevier.com/locate/lithos

Early Cretaceous dioritic rocks in the Tongling region, eastern China: Implications for the tectonic settings

Jiancheng Xie [a,b], Xiaoyong Yang [a,*], Weidong Sun [c,**], Jianguo Du [d]

[a] CAS Key Laboratory of Crust–Mantle Materials and Environments, School of Earth and Space Sciences, University of Science and Technology of China, Hefei 230026, China
[b] School of Resource and Environmental Sciences, Hefei University of Technology, Hefei, 230009, China
[c] CAS Key Laboratory of Mineralogy and Metallogeny, Guangzhou Institute of Geochemistry, Guangzhou 510640, China
[d] Anhui Academy of Geological Survey, Hefei 230001, China

ARTICLE INFO

Article history:
Received 15 April 2011
Accepted 8 May 2012
Available online 17 May 2012

Keywords:
Adakite
Slab melting
Ridge subduction
Copper
Tongling dioritic rocks
The Lower Yangtze metallogenic belt

ABSTRACT

The Tongling district in the Lower Yangtze River belt is one of the most important Cu-polymetal producers in China. Copper–Au deposits in the region are closely related to Early Cretaceous dioritic intrusions, which can be classified into three rock associations: pyroxene diorite–pyroxene monzodiorite, quartz diorite–quartz monzodiorite and granodiorite. The dioritic rock series (SiO_2 = 54.6–64.5 wt.%) are calc-alkaline, with high Al_2O_3 (>15.4 wt.%), Ba (Ba>700 ppm) and Sr concentrations (~920 ppm in average), and low Y and Yb concentrations, all of which are typical for adakite. Geochemical characteristics suggest that the Tongling adakitic rocks are genetically related to slab melting and subsequent interaction with the mantle, likely during a ridge subduction along the Lower Yangtze River Belt in the Early Cretaceous. Geothermometers show high formation temperatures of 800–900 °C, which is consistent with interaction with the asthenosphere mantle as indicated. The relatively low $\varepsilon_{Nd}(t)$ values (−11.2 to −16.7) and high $(^{87}Sr/^{86}Sr)_i$ ratios (0.7067 to 0.7095) may be plausibly interpreted by contamination of enriched mantle materials and/or continental crust. The Tongling dioritic rocks are characterized by high radiogenic Pb isotopes with $(^{206}Pb/^{204}Pb)_i$ = 17.80–18.56, $(^{207}Pb/^{204}Pb)_i$ = 15.46–15.60, and $(^{208}Pb/^{204}Pb)_i$ = 37.92–38.48, which mostly plot in the field of MORB, near the intersection of EM-1 and EM-2, and are clearly different from those of the upper and lower continental crust and Dabie adakites. These exclude major contamination from the continental crust. Given that eastern China has both EM-1 and EM-2 types of enriched mantle, whereas the Tongling region is located near the transition from EM-1 to EM-2, the enriched Sr–Nd isotopic characteristics of Tongling adakites are best explained by slab melts with assimilation of enriched mantle components.

1. Introduction

The Tongling region of Anhui Province is an important ore district of the famous Lower Yangtze River metallogenic belt (LYRB) in central eastern China, and also a good example of skarn deposits in China (Chang et al., 1991; Pan and Dong, 1999; Zhai et al., 1996) (Fig. 1a). Metal deposits are closely associated with and genetically related to the Early Cretaceous dioritic rocks in the region (Chang et al., 1991; Ling et al., 2009, 2011; Liu et al., 2010; Sun et al., 2010, 2011; Wang et al., 2003a; Xie et al., 2009; Xing and Xu, 1996; Yang and Lee, 2011; Yang et al., 2011; Zhai et al., 1996) (Fig. 1b). The petrogenesis of dioritic rocks in the Tongling region, however, has been a subject of much debate with a number of competing models: (1) the mixing of mantle-derived and crust-derived magmas, or assimilation and fractional crystallization process of mantle-derived magmas, with major contributions from an ancient crustal component (Chen and Jahn, 1998; Chen et al., 1993; Xing and Xu, 1996); (2) partial melting of lower crust materials in the Yangtze continental block (Zhang et al., 2001); (3) rocks with $SiO_2 \leq 55\%$ were produced by crystallization of basaltic magmas derived from an enriched mantle, with limited assimilation of lower crustal materials, whereas rocks with $SiO_2 > 55\%$ were generated by the mixing of mantle-derived basaltic magmas and adakite-like magmas derived from the melting of basaltic lower crust due to heating of underplating shoshonitic magmas (Wang et al., 2003a,b); and (4) ridge subduction induced magmas modified by enriched mantle components and crustal assimilation (Ling et al., 2009, 2011; Sun et al., 2010).

This paper focuses on the petrology and geochemistry of dioritic intrusions closely associated with Cu–Au–Fe ore deposits in the Tongling region (e.g., Tongguanshan, Shizishan, Fenghuangshan, Shatanjiao and Xinqiao ore fields) (Fig. 1b). These ore deposits are mainly typical skarn-type Cu (Au) mineralization with the exception of the Xinqiao deposit, which is Cu–Au–S–Fe mineralization attributed either to synorogenic remobilization of a stratiform sulfide deposit (e.g., Xu and

* Correspondence to: X. Yang, CAS Key Laboratory of Crust–Mantle Materials and Environments, School of Earth and Space Sciences, University of Science and Technology of China, Hefei 230026, China.
** Correspondence to: W. Sun, CAS Key Laboratory of Mineralogy and Metallogeny, Guangzhou Institute of Geochemistry, Guangzhou 510640, China.
E-mail addresses: xyyang555@163.com (X. Yang), weidongsun@gig.ac.cn (W. Sun).

0024-4937/$ – see front matter © 2012 Published by Elsevier B.V.
doi:10.1016/j.lithos.2012.05.008

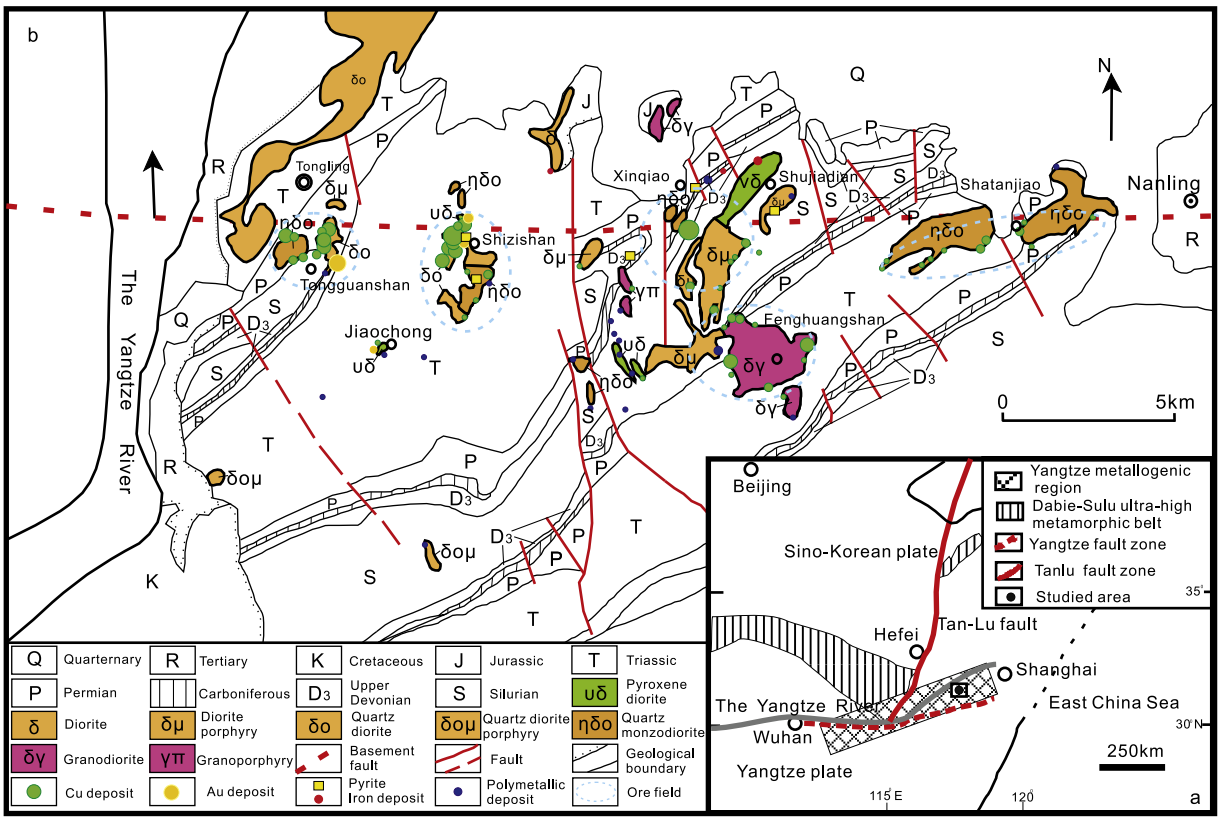

Fig. 1. Geological sketch map of the Tongling metallogenic district, eastern China. Modified after Xie et al. (2009).

Zhou, 2001), or to magmatic origin (Xie et al., 2009). The geochemical characteristics of the ore-bearing dioritic rocks in the Tongling region are summarized and discussed here, drawing upon systematical analyses of major elements, trace elements and Sr–Nd–Pb isotopes together with data collected from the literature. Our results support the model of partial melting of the subducted oceanic crust, likely during a ridge subduction.

2. Regional geological setting

The Tongling region is situated in the Yangtze craton in central eastern China (Fig. 1a). Cambrian to middle Triassic sedimentation developed on a stable Precambrian basement, forming a thick sedimentary sequence that became country rocks for later Cu, Au, and Fe skarn deposits (Chang et al., 1991) (Fig. 1b). The Indosinian tectonic setting of the region is dominated by compression, forming a series of NE trending folds and faults, likely associated with the Triassic collision between the South and North China blocks (Li et al., 1993; Sun et al., 2002). During the Yanshanian period (Jurassic/Cretaceous), this region became active again, in an event that has long been interpreted as an intraplate deformational stage with abundant magmatism (Chang et al., 1991). Intrusions of abundant intermediate felsic rocks and associated hydrothermal activity produced numerous metal deposits (Chang et al., 1991) (Fig. 1b).

Marine deposits in the Tongling region, which include clastic sedimentary rocks, carbonates, and evaporates, occurred from the Silurian through to the Middle Triassic, with the exception of the Middle–Late Devonian. Mesozoic sedimentary–volcanic basins are widely distributed on these marine deposits (Chang et al., 1991) (Figs. 1b and 2). The strata, which are closely related to the metal deposits, are Carboniferous carbonate, Permian limestone, black shale, and Triassic carbonate and argillaceous rocks (Chang et al., 1991; Pan and Dong, 1999) (Fig. 2).

Mesozoic magmatic rocks (J–K) are abundant in the region, forming more than 70 intrusions. These intrusions are mostly located within the Lower Yangtze magmatic metallogenic belt controlled by the EW trending Tongling–Nanling deep fault (Fig. 1b) (Chang et al., 1991). Three main rock associations have been identified: (i) pyroxene diorite–pyroxene monzodiorite association, which is closely related to regional gold mineralization; (ii) quartz diorite–quartz monzodiorite association, the most important magmatic rock series in the Tongling region and primarily related to Cu–Au–Fe mineralization; and (iii) granodiorite association, which is closely related to copper-polymetallic deposits (Fig. 1b). High-precision zircon U–Pb (SHRIMP and LA-ICP-MS) results for intrusive rocks in the Tongling region have shown that all the three rock associations formed in the Early Cretaceous (mainly 145–137 Ma; Wu et al., 2008; J.C. Xie et al., 2008; Xie et al., 2009; Xu et al., 2004; Yang et al., 2011).

Deposits so far discovered in the Tongling district are grouped into several ore fields, such as Tongguanshan, Shizishan, Xinqiao, Fenghuangshan and Shatanjiao (Fig. 1b). These deposits show a clear spatial zonation with a central Cu–Au–Fe–S deposit belt and the south and north polymetallic deposit belts (Fig. 1b). The Tongling district is characterized by skarn- and strata-bound-type mineralization, whereas porphyry-type Cu deposits are generally minor and occurs in the deeper parts of a few skarn deposits (Chang et al., 1991; Pan and Dong, 1999). In some deposits, skarn and porphyry mineralization developed simultaneously (Chang et al., 1991). Moreover, there also exist a number of bedded skarn and/or bedded massive sulfide ore bodies. The presence of skarn and strata-bound deposits in the same system has caused much debate as to whether those deposits were associated with igneous (Chang et al., 1991; Ling et al., 2009, 2011; Mao et al., 2006; Pan and Dong, 1999; Xie et al., 2009; Yang and Lee, 2011; Zhou et al., 2010) or sedimentary rocks (Gu and Fu, 1999; Guo et al., 2010; Lu et al., 2008; Xu and Zhou, 2001). Recent studies have shown that the porphyry and skarn deposits have molybdenite Re–Os ages identical to the strata-

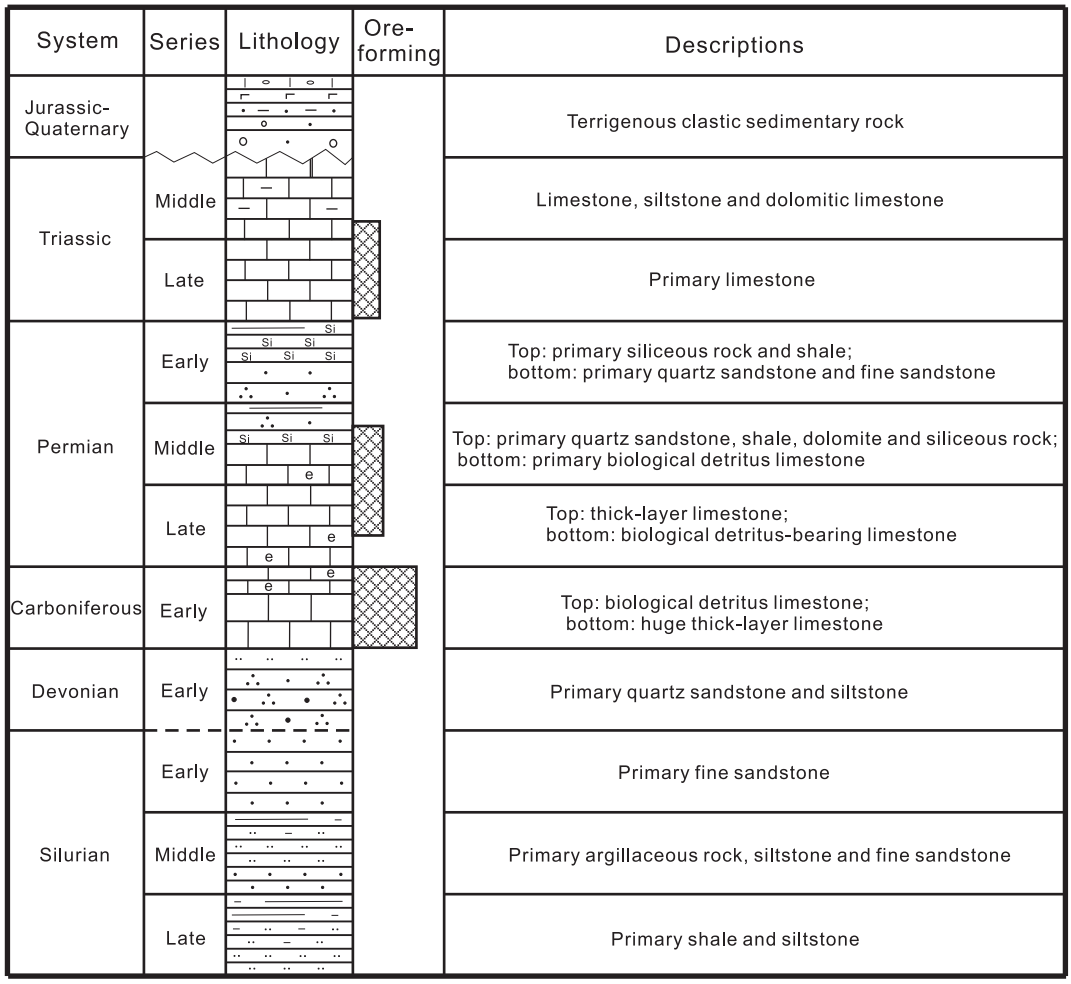

Fig. 2. Stratigraphic section of the Tongling metallogenic district, eastern China.
Modified after Xie et al. (2009).

bound deposits (Mao et al., 2006; Sun et al., 2003). These ore deposits all formed in the Early Cretaceous (143–134 Ma; Mao et al., 2006; Sun et al., 2003), supporting the view that they are genetically related to Early Cretaceous igneous rocks (Wu et al., 2008; J.C. Xie et al., 2008; Xie et al., 2009; Xu et al., 2004; Yang et al., 2011).

3. Petrography

The dioritic rocks mainly consist of pyroxene diorite–pyroxene monzodiorite association, quartz diorite–quartz monzodiorite association and granodiorite association. These rocks are gray in color with fine grain or porphyritic textures. The samples were collected from fresh outcrops and drill cores in the Tongling metallogenic district. Characteristics of samples from intrusive rocks are listed in Table 1.

3.1. Pyroxene diorite–pyroxene monzodiorite association

Rock types of this association are primary pyroxene diorite (diorite porphyry) and pyroxene monzodiorite (diorite porphyry). Pyroxene diorite is dark gray in color with porphyritic texture. Phenocrysts mainly consist of plagioclase, augite, hornblende and alkali-feldspar (Fig. 3a). Plagioclase develops multiple twins and zone texture, with modal proportions of 15%. The grain size of plagioclase phenocrysts ranges from 1×2 mm to 2×4 mm. Alkali-feldspar has Carlsbad twins with modal proportions of 5%. Hornblende phenocrysts (about 10%) are mostly brown in color with a few green pleochroic grains. Augite (about 15 modal %) is subhedreal to euhedral with zonations. The matrix is plagioclase, hornblende and augite, with a total proportion of ~40%.

3.2. Quartz diorite–quartz monzodiorite association

The quartz diorite–quartz monzodiorite rock association, which consists mainly of quartz diorite, quartz monzodiorite and diorite porphyrite, is the most abundant rock type in the Tongling region.

Quartz monzodiorite is offwhite with a fine grained texture. The typical modal mineralogy is ~40% plagioclase, ~35% alkali-feldspar, ~10% green hornblende, ~8–15% quartz, and traces of sulfide minerals, apatite and titanite (Fig. 3b and c). Plagioclase is subhedral to euhedral, with multiple twins, rims of albite and fragmentation phenomenon. Alkali-feldspar has Carlsbad twin, poikilitic texture, with rims of albite. Hornblende encloses alkali-feldspar, biotite, apatite and metal minerals, implying magma mixing.

Quartz diorite is gray in color, displays fine grained texture, and consists of plagioclase (66%–71%), K-feldspar (3%–6%), quartz (1%–7%), hornblende (10%–17%), and biotite (1%–3%), with a few traces of metal minerals, apatite, zircon and titanite (Fig. 3d and e).

3.3. Granodiorite association

The granodiorite association consists of granodiorite and granodiorite porphyrite. Granodiorite (Fig. 3f) is gray in color with subhedral grain texture and massive structure, consisting mainly of plagioclase (45–60%), hornblende (10–15%), quartz (15–20%), K-feldspar (10–15%), biotite

Table 1
Characteristics of samples from dioritic rocks in Tongling region.

Sample no	Location	Outcrop area (km^2)	Shape	Lithology	Wallrock	Alteration	Related deposit
TLMS01	Shujiadian E117°57′13.7″, N30°54′41.3″	0.5	Irregular triangle, stock	Pyroxene monzodiorite	Devonian, Carboniferous and Permian	Fresh	Cu deposit
TLXDGS01	Shizishan E117°53′18.6″, N30°55′26.4″	<0.5	Irregular stock	Quartz diorite	Triassic limestone and dolomite	Fresh	Cu–Au deposit
TLBMS01	Shizishan E117°53′26.2″, N30°54′57.0″	0.3	Dyke	Pyroxene diorite	Triassic limestone and dolomite	Fresh	Au deposit
TLJGS01	Shizishan E117°54′06.9″, N30°54′28.8″	1.1	Small-sized mushroom, stock	Quartz monzodiorite	Triassic limestone and dolomite	Fresh, weakly altered	Cu–Au deposit
TLBC02	Shizishan E117°53′29.4″, N30°55′47.6″	About 0.3	Ellipsoidal stock	Quartz monzodiorite	Triassic limestone and dolomite	Fresh	Au deposit
TLSTJ02	Shatanjiao E118°11′15.3″, N30°55′49.7″	About 12	Irregular long circle, stock	Quartz monzodiorite	Triassic limestone and dolomite	Fresh	Cu–Au deposit
TLXQT02	Xinqiao E118°01′39.4″, N30°56′06.7″	4	Irregular stock	Diorite porphyry	Silurian siltstone	Fresh	Cu–Au deposit
TLTEBD01	Tongguanshan E117°49′54.3″, N30°54′50.8″	0.8	irregular round, stock	quartz diorite	Permian limestone	fresh	Cu–Au deposit
TLHS01	Tongguashan E117°49′57.7″, N30°55′50.3″	0.35	Irregular long circle, apophyses	Diorite porphyry	Triassic limestone and dolomite	Fresh	Cu–Au deposit
TLWLS01	Shizishan E117°53′28.1″, N30°54′45.1″	0.7	Irregular stock	Quartz monzodiorite	Triassic limestone and dolomite	Fresh	Cu–Au deposit
TLFHS01	Fenghuangshan E118°01′ 50.1″, N30°52′29.0″	9.5	Ellipsoidal stock	Quartz diorite	Devonian–Triassic	Fresh	Cu–polymetallic deposit
TGS16	Tongguanshan E117°48′51.5″, N30°54′27.7″	1.5	Long circle, stock	Quartz diorite	Devonian, Carboniferous and Permian	Fresh	Cu–Au deposit
TLJKL01	Tongguanshan E117°47′09.8″, N30°54′51.0″	5	Irregular round, stock	Quartz monzodiorite	Triassic limestone and dolomite	Fresh	Cu–Au deposit
TLHC01	Shizishan E117°53′11.2″, N30°54′24.3″	<0.5	Ellipsoidal stock	Quartz monzodiorite	Triassic limestone and dolomite	Fresh	Cu–Au deposit
TLQTY01	Shujiadian E118°07′31.7″, N30°54′58.1″	2?	Irregular long circle, stock	Granodiorite	Silurian siltstone	Fresh	Cu–Au deposit

(0–5%), and accessory minerals including titanite, magnetite, apatite and zircon. Plagioclase with grain sizes of 0.3–1.0 mm is subhedral to euhedral, with multiple twins, rims of albite and fragmentation phenomenon. Hornblende with grain size of 0.3–0.8 mm is semi-automorphic to automorphic texture. Quartz is anhedral with grain size of ~0.2 mm. K-feldspar is semi-automorphic to anhedral with a grain size of generally less than 0.2 mm.

4. Analytical methods

Major elements were analyzed at the Physics and Chemistry Laboratory Center of the University of Science and Technology of China; rare earth and other trace elements were analyzed at ALS Laboratory Group — an Australian ICP-MS analytical lab in Guangzhou. Major elements were analyzed on a PHILIPS PW-2404 X-fluorescence spectrometer. The analyzed samples were first fused in $Li_2B_4O_7$ flux with a sample to flux ratio of 1:5 at temperatures of 1150–1250 °C. Then, the fused samples were made into glass disks for analyses. The accuracy was better than 1%. Trace and rare earth elements of the samples were determined using ICP-MS on an ELEMENT-2 mass spectrometer. Whole-rock powders (50 mg) were dissolved in sealed Teflon beakers with mixed HNO_3 + HF for 1–2 days. Then the beakers were opened and $HClO_4$ was added for further digestion. After evaporation, a 5% HNO_3 solution was used to dilute the sample to a determined volume of 50 ml for final measurement. Rock standards of the GBW series were analyzed together with samples to check the external reproducibility. The analysis accuracy was estimated to be better than 10%. The major, rare earth and other trace element concentrations determined are given in Table 2.

The Rb, Sr, Sm, Nd and Pb data were determined using a MAT-262 mass spectrometer in the Laboratory for Chemical Geodynamics of the University of Science and Technology of China. Total procedure blanks were 0.4 ng for Sr and 50 pg for Nd. The mass fractionations of Sr, Sm and Nd isotopic ratios were calibrated using $^{86}Sr/^{88}Sr = 0.1194$, $^{149}Sm/^{152}Sm = 0.516858$, and $^{146}Nd/^{144}Nd = 0.7219$, respectively. Detailed analytical procedures are similar to those described in Foland and Allen (1991). Standards analyzed along with samples were as follows: NBS987 of $^{87}Sr/^{88}Sr = 0.710250 \pm 12$ (2σ); and La Jolla of $^{143}Nd/^{144}Nd = 0.511860 \pm 12$ (2σ). Lead was purified using conventional anion-exchange method using HBr as an eluant. The whole procedure blank for Pb is 0.05–0.1 ng. Fractionation of Pb isotopes during mass spectrometry analysis was calibrated against a standard, NBS981. The average isotopic composition for NBS981 measured during the course of this study was $^{206}Pb/^{204}Pb = 16.9344 \pm 0.0013$ (2σ), $^{207}Pb/^{204}Pb = 15.4460 \pm 0.0013$ (2σ), and $^{208}Pb/^{204}Pb = 36.6054 \pm 0.0033$ (2σ). The precision of Pb isotope data on the mass spectrometry was better than 0.1%. Isotopic data are given in Tables 3 and 4.

5. Results

5.1. Major and trace elements

The Tongling dioritic rocks show large compositional variations, with SiO_2 contents ranging from 54.6 to 64.5 wt.% (Table 2). The total alkali contents of ($Na_2O + K_2O$) vary from 6.70 to 8.48 wt.%, showing characteristics of the sub-alkaline series (Fig. 4a). The low A.R. values of 1.84–2.63 [A.R. = ($Al_2O_3 + CaO + Na_2O + K_2O$)/($Al_2O_3 + CaO - Na_2O - K_2O$)] show calc-alkaline characteristics (Fig. 4b). The Tongling dioritic rocks also have TiO_2 (0.43–1.08 wt.%), P_2O_5 (0.14–0.57 wt.%), Th contents (4.17–11.7 ppm), and Th/Ce ratios (0.08–0.15), comparable to adakites derived from partial melting of subducted young oceanic crust (Aguillón-Robles et al., 2001; Defant and Drummond, 1990; Drummond et al., 1996; Stern and Kilian, 1996). All the Tongling rocks formed at high temperatures, about 800–900 °C, as estimated from P_2O_5 and TiO_2 contents using conventional geothermometers (Fig. 5a and b) (Green and Pearson, 1986; Harrison and Watson, 1984).

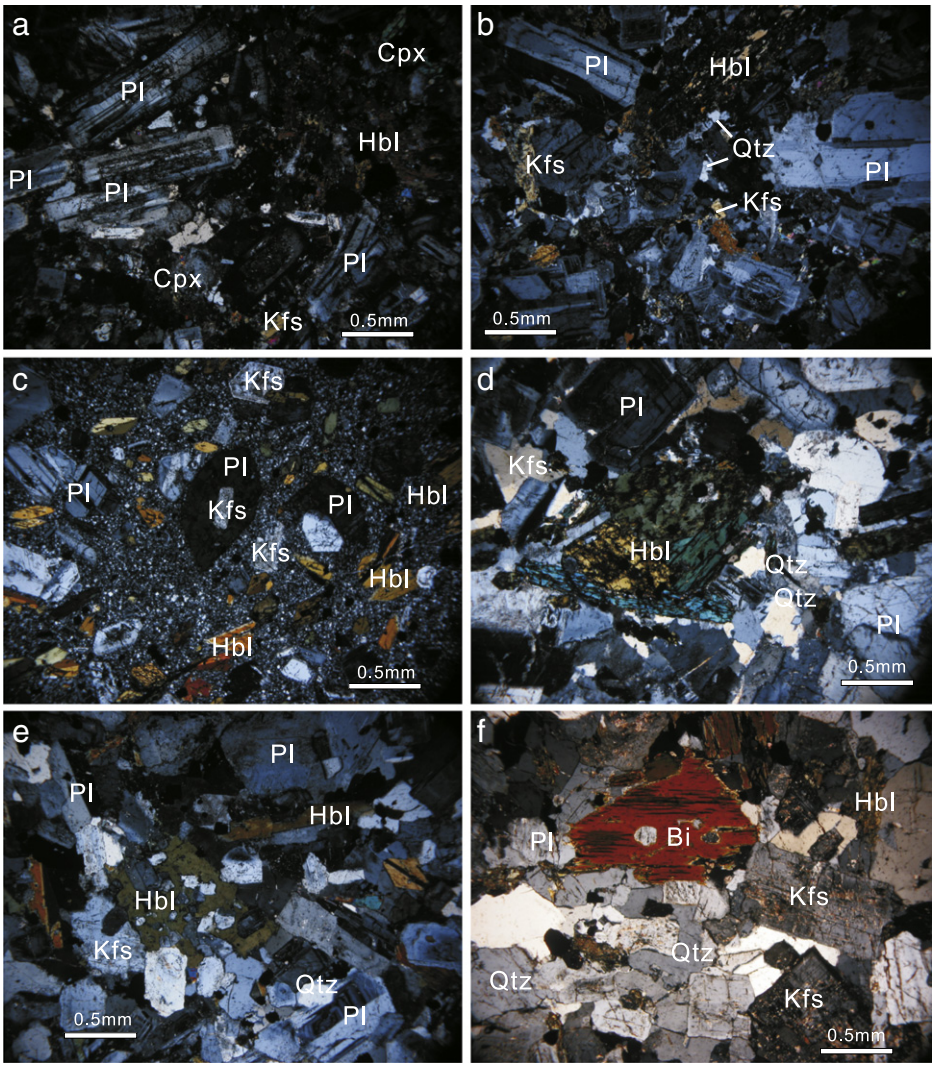

Fig. 3. Photomicrographs illustrating minerals of the dioritic rocks in the Tongling region. All the images were taken using a Leica microscope under polarized light conditions. The scale bar for each image is 0.50 mm. Abbreviations in the images: Pl, plagioclase; Kfs, potassic feldspar; Hbl, hornblende; and Bi, biotite. a — Pyroxene diorite, which mainly consists of plagioclase, pyroxene, hornblende and alkali-feldspar, has different grain texture–porphyritic texture; b and c — plagioclase, alkali-feldspar, hornblende and quartz are the major mineral components of quartz monzodiorite, note the zoning texture of plagioclase and packing texture (plagioclase packing alkali-feldspar and hornblende); d and e — plagioclase, potassic feldspar, hornblende and quartz are the major mineral components of quartz diorite, note the hornblende packing alkali-feldspar and plagioclase; and f — granodiorite which mainly consists of plagioclase, hornblende, quartz, K-feldspar and biotite has half-automorphic grain texture and massive structure.

The Tongling dioritic samples have geochemical features similar to those of adakites: high Al_2O_3 (>15.4 wt.%), high Ba (Ba>700 ppm) and Sr concentrations (>629 ppm, average 920 ppm), high Sr/Y (most>40), La/Yb (>20), and low Yb (0.80–2.59 ppm, mean 1.75 ppm) and Y concentrations (9.80–24.4 ppm, average 17.6 ppm) (Defant and Drummond, 1990; Kay and Kay, 1993; Martin, 1999; Martin et al., 2005). As shown in Fig. 6a and b, most of the diorites plot in the adakite field with high Sr/Y and low Y similar to other Mesozoic adakites observed in eastern China, e.g., LYRB (Gao et al., 2006; Liu et al., 2010; Wang et al., 2003a,b; 2004a,b; 2006; 2007b; G.Q. Xie et al., 2008; Xu et al., 2002; Y.L. Wang et al., 2004), and the Dabie orogen (Huang et al., 2008; Wang et al., 2007a).

The Tongling dioritic rocks have 109–240 ppm of total REE and display coherent REE patterns characterized by relative enrichments of LREE and nearly flat HREE ($(La/Yb)_N$=12.2–26.5; Table 2), with weak negative Eu anomalies (average Eu^*/Eu=0.87) (Fig. 7a). On a N-MORB normalized trace element plot, Tongling dioritic rocks show coherent patterns, with pronounced negative Nb, Ta, Ti anomalies and a positive Sr anomaly (Fig. 7b). Both the REE pattern and N-MORB normalized diagram are comparable to those of adakites from the Austral Volcanic Zone (AVZ) and circum-Pacific adakites (Fig. 7a and b), which are believed to be formed through partial melting of the subducted oceanic crust (Liu et al., 2010; Stern and Kilian, 1996; Sun et al., 2012).

5.2. Sr–Nd–Pb isotopes

The Tongling dioritic rocks show high $(^{87}Sr/^{86}Sr)_i$ values of 0.7067–0.7095 and low $\varepsilon_{Nd}(t)$ values of −11.2 to −16.7 (Table 3), which are similar to the values of other adakitic rocks from the LYRB (Fig. 8) (Chen et al., 1993; Gao et al., 2006; Liu et al., 2010; Wang et al., 2003a,b; 2004a,b; 2006; 2007b; G.Q. Xie et al., 2008; Xu et al., 2002). In a $\varepsilon_{Nd}(t)$ versus $(^{87}Sr/^{86}Sr)_i$ diagram, all samples of the Tongling dioritic rocks roughly define a negative correlation line, mostly plotted near the fields of marine sediments and OIB (Hofmann, 2003). They are distinctly different from Dabie adakites derived from partial melting of delaminated (generally high-Mg) or thickened lower crust (usually low-Mg) (Huang et al., 2008; Ling et al., 2011; Wang et al., 2007a), but are similar to those of the Early Cretaceous adakitic rocks from the LYRB (Fig. 8).

The Tongling dioritic rocks are characterized by high radiogenic Pb isotopes with $(^{206}Pb/^{204}Pb)_i$=17.80–18.56, $(^{207}Pb/^{204}Pb)_i$=15.46–

Table 2
Major and trace elements compositions of the dioritic rocks in the Tongling region.
Normalizing values after Sun and McDonough (1989).

Sample	TLMS01	TLXDGS01	TLBMS01	TLJGS01	TLBC02	TLSTJ02	TLXQT02	TLTEBD01	TLHS01	TLWLS01	TLFHS01	TGS16	TLJKL01	TLHC01	TLQTY01
Major oxides (wt.%)															
SiO_2	54.6	57.3	57.6	59.1	59.5	59.8	60.9	61.1	61.5	62.1	62.4	63.0	63.4	64.1	64.5
TiO_2	1.08	0.95	0.96	0.86	0.78	0.71	0.57	0.74	0.71	0.65	0.62	0.54	0.57	0.59	0.43
Al_2O_3	16.4	16.7	16.9	16.7	16.1	16.8	17.0	16.3	16.1	16.3	15.8	16.3	16.6	15.4	15.6
Fe_2O_3	5.24	6.15	6.44	6.47	5.42	5.28	6.49	5.13	5.79	5.21	4.93	4.56	4.72	3.28	2.87
MnO	0.08	0.08	0.16	0.16	0.07	0.09	0.06	0.10	0.11	0.09	0.07	0.08	0.09	0.05	0.02
MgO	3.50	2.51	2.30	2.26	2.08	2.04	1.84	2.09	2.14	1.75	1.68	1.50	1.43	1.49	1.05
CaO	6.89	5.83	6.37	5.93	4.89	5.31	1.88	5.65	4.57	4.88	4.34	4.42	4.66	4.99	3.31
Na_2O	4.46	3.67	4.62	3.92	4.08	4.78	4.83	4.05	4.17	4.27	4.04	4.60	4.53	4.27	4.85
K_2O	2.61	3.03	2.98	2.77	3.29	2.28	3.65	3.21	2.66	2.74	3.04	2.55	2.44	3.42	3.35
P_2O_5	0.57	0.41	0.33	0.35	0.31	0.32	0.20	0.29	0.35	0.27	0.26	0.24	0.25	0.23	0.14
LOI	3.51	2.88	0.49	1.57	2.73	1.04	1.57	0.98	2.24	1.14	2.14	0.68	0.58	1.67	3.4
Total	99.0	99.5	99.1	100.0	99.2	98.5	99.0	99.6	100.4	99.4	99.4	98.5	99.3	99.5	99.6
Trace elements (ppm)															
Ba	646	717	747	721	795	742	1145	928	870	913	871	918	934	952	868
Cr	20.0	10.0	<10	<10	30.0	10.0	20.0	10.0	10.0	70.0	10.0	10.0	10.0	10.0	20.0
Cu	<5	61.0	28.0	19.0	167	140	<5	18.0	8.00	6.00	208	12.0	6.00	156	53.0
Ga	19.9	23.3	22.6	21.4	22.6	23.1	23.9	21.7	22.9	21.9	22.5	23.8	23.4	20	23.2
Hf	5.40	5.90	5.60	4.80	5.50	6.60	4.50	5.60	5.80	5.10	5.30	5.40	5.00	4.50	5.20
Nb	14.7	14.7	14.5	12.5	14.1	14.4	11.2	14.6	15.2	13.1	15.3	12.9	12.4	12.8	12.9
Ni	24.0	10.0	6.00	7.00	18.0	6.00	11.0	9.00	8.00	52.0	23.0	12.0	10.0	10.0	14.0
Pb	23.0	14.0	19.0	13.0	15.0	11.0	7.00	29.0	19.0	17.0	13.0	12.0	15.0	15.0	15.0
Rb	64.7	86.1	74.7	75.1	92.2	53.6	140	87.3	74.0	81.8	134	77.7	58.2	70.3	89.9
Sr	1225	887	871	776	819	1100	629	894	863	914	792	1050	1080	841	996
Ta	1.10	1.00	0.90	0.80	0.90	0.80	0.70	1.00	1.10	0.90	1.20	0.80	0.80	1.00	0.80
Th	10.6	9.22	11.7	10.6	9.50	6.92	4.17	11.5	9.48	7.88	8.93	9.01	6.63	9.72	7.48
U	2.96	2.23	3.19	2.72	2.53	2.76	1.43	2.25	2.38	2.20	2.95	2.79	1.89	2.69	2.38
V	148	126	139	122	103	90.0	79.0	97.0	86.0	85.0	81.0	64.0	68.0	82.0	49.0
Y	24.4	20.9	20.8	20.7	20.0	18.0	10.0	20.8	21.5	16.6	18.0	13.1	13.3	15.3	9.80
Zr	211	236	219	183	220	251	173	216	223	189	204	201	188	163	198
La	46.8	43.8	45.2	40.4	40.8	42.2	22.8	40.9	53.9	37.1	41.9	36.9	35.4	35.6	33.0
Ce	91.1	86.4	84.5	77.5	80.4	86.1	43.8	78.5	104	71.3	81.0	68.6	67.6	66.6	64.0
Pr	10.6	10.2	9.81	8.90	9.39	10.2	5.51	9.09	11.9	8.14	9.28	7.92	7.89	7.54	7.31
Nd	39.8	37.6	35.7	32.4	34.5	38.6	22.0	33.9	43.2	29.6	33.4	29.6	29.2	27.1	27.1
Sm	6.99	6.79	6.28	5.95	6.15	6.65	4.18	6.06	7.24	5.34	5.77	5.3	5.35	4.94	4.84
Eu	1.81	1.83	1.79	1.57	1.62	1.72	1.51	1.56	1.84	1.47	1.47	1.41	1.43	1.28	1.11
Gd	6.42	5.95	5.79	5.45	5.48	5.99	3.60	5.61	6.62	4.84	5.27	4.42	4.43	4.47	3.88
Tb	0.90	0.83	0.81	0.79	0.77	0.77	0.47	0.79	0.87	0.67	0.72	0.59	0.58	0.57	0.45
Dy	4.94	4.15	4.14	4.15	4.03	3.68	2.18	4.23	4.5	3.37	3.63	2.7	2.88	3.07	2.02
Ho	0.99	0.83	0.87	0.82	0.82	0.69	0.39	0.82	0.85	0.65	0.71	0.51	0.54	0.62	0.37
Er	2.86	2.33	2.29	2.33	2.26	1.88	1.02	2.33	2.49	1.9	2.07	1.38	1.41	1.75	0.98
Tm	0.39	0.31	0.34	0.31	0.33	0.22	0.13	0.33	0.34	0.24	0.3	0.19	0.2	0.25	0.12
Yb	2.59	2.03	2.21	2.20	2.00	1.69	0.80	2.05	2.19	1.62	1.94	1.25	1.23	1.57	0.84
Lu	0.38	0.3	0.36	0.36	0.33	0.25	0.11	0.32	0.34	0.25	0.29	0.19	0.21	0.25	0.12
$\sum$	217	203	200	183	189	201	109	186	240	166	188	161	158	156	146
$(La/Yb)_N$	12.2	14.6	13.8	12.4	13.8	16.9	19.3	13.5	16.6	15.5	14.6	19.9	19.4	15.3	26.5
Eu*/Eu	0.83	0.88	0.91	0.84	0.85	0.83	1.19	0.82	0.81	0.88	0.81	0.89	0.90	0.83	0.78
Sr/Y	50.2	42.4	41.9	37.5	41.0	61.1	62.9	43.0	40.1	55.1	44.0	80.2	81.2	55.0	102

$Eu^*/Eu = Eu_N/(Sm_N \times Gd_N)^{1/2}$.

Table 3
Nd and Sr isotopic compositions of the dioritic rocks from Tongling region.

Sample no	Rb (ppm)	Sr (ppm)	$^{87}Rb/^{86}Sr$	$^{87}Sr/^{86}Sr$	2σ	$(^{87}Sr/^{86}Sr)_i$	Sm (ppm)	Nd (ppm)	$^{147}Sm/^{144}Nd$	$^{143}Nd/^{144}Nd$	$(^{143}Nd/^{144}Nd)_i$	2σ	$\varepsilon_{Nd}(t)$
TLMS01	64.7	1225	0.1491	0.707241	14	0.706946	6.99	39.8	0.11062	0.512149	0.512048	15	−11.2
TLXDGS01	86.1	887	0.2740	0.707644	13	0.707103	6.79	37.6	0.11374	0.512072	0.511969	15	−12.7
TLBMS01	74.7	871	0.2421	0.707566	12	0.707088	6.28	35.7	0.11079	0.512118	0.512017	15	−11.8
TLJGS01	75.1	776	0.2732	0.707259	12	0.706719	5.95	32.4	0.11566	0.512092	0.511987	12	−12.3
TLBC02	92.2	819	0.3177	0.708270	13	0.707642	6.15	34.5	0.11227	0.512032	0.511930	14	−13.5
TLSTJ02	53.6	1100	0.1375	0.708722	15	0.708450	6.65	38.6	0.10851	0.512073	0.511974	13	−12.7
TLXQT02	140	629	0.6282	0.709442	15	0.708201	4.18	22.0	0.11967	0.511998	0.511889	14	−14.2
TLTEBD01	87.3	894	0.2756	0.707314	14	0.706777	6.06	33.9	0.11259	0.511962	0.511860	15	−14.9
TLHS01	74	863	0.2420	0.709629	14	0.709151	7.24	43.2	0.10556	0.511866	0.511770	14	−16.7
TLWLS01	81.8	914	0.2526	0.707259	12	0.706767	5.34	29.6	0.11363	0.512027	0.511924	14	−13.6
TLFHS01	134	792	0.4775	0.710239	15	0.709295	5.77	33.4	0.10881	0.511831	0.511732	14	−15.6
TGS16	77.7	1050	0.2089	0.707616	11	0.707203	5.30	29.6	0.11277	0.511944	0.511841	12	−15.2
TLJKL01	58.2	1080	0.1521	0.707183	13	0.706887	5.35	29.2	0.11540	0.511958	0.511853	12	−14.9
TLHC01	70.3	841	0.2359	0.709998	12	0.709532	4.94	27.1	0.11481	0.511989	0.511885	15	−14.3
TLQTY01	89.9	996	0.2548	0.708743	14	0.708240	4.84	27.1	0.11249	0.512029	0.511927	10	−13.6

Initial Sr and Nd isotopic ratios for Tongling samples are calculated based on t = 139 Ma (Yang et al., 2011).

Table 4
Pb isotopic compositions of the dioritic rocks from Tongling region.

Sample no	U (ppm)	Th (ppm)	Pb (ppm)	$^{206}Pb/^{204}Pb$	2σ	$^{207}Pb/^{204}Pb$	2σ	$^{208}Pb/^{204}Pb$	2σ	$(^{206}Pb/^{204}Pb)_t$	$(^{207}Pb/^{204}Pb)_t$	$(^{208}Pb/^{204}Pb)_t$
TLMS01	2.96	10.55	23	18.3720	12	15.5163	13	38.2572	16	18.235	15.560	38.221
TLXDGS01	2.23	9.22	14	18.2514	12	15.4813	13	38.3063	13	18.072	15.523	38.180
TLBMS01	3.19	11.7	19	18.5200	12	15.5354	13	38.3194	14	18.329	15.576	38.212
TLJGS01	2.72	10.55	13	18.5925	13	15.5590	13	38.6008	18	18.342	15.597	38.404
TLBC02	2.53	9.5	15	18.2602	11	15.4862	13	38.3145	14	18.068	15.527	38.200
TLSTJ02	2.76	6.92	11	18.6519	13	15.5581	13	38.5415	16	18.344	15.593	38.427
TLXQT02	1.43	4.17	7	18.4592	11	15.5286	13	38.3671	14	18.217	15.567	38.269
TLTEBD01	2.25	11.45	29	18.1640	12	15.5070	13	38.2825	16	18.098	15.554	38.276
TLHS01	2.38	9.48	19	18.1551	12	15.4573	13	38.1655	15	18.023	15.501	38.112
TLWLS01	2.2	7.88	17	18.1660	11	15.4842	13	38.1394	14	18.029	15.528	38.102
TLFHS01	2.95	8.93	13	18.8393	11	15.5107	13	38.6238	14	18.564	15.547	38.483
TGS16	2.79	9.01	12	18.0923	12	15.4204	13	38.0890	18	17.814	15.457	37.922
TLJKL01	1.89	6.63	15	17.9365	13	15.4461	13	37.9534	16	17.804	15.490	37.926
TLHC01	2.69	9.72	15	18.3340	12	15.4997	12	38.3793	13	18.127	15.540	38.258
TLQTY01	2.38	7.48	15	18.5269	12	15.5510	13	38.4843	14	18.348	15.592	38.430

For the whole-rock of the Tongling samples, $(^{206}Pb/^{204}Pb)_t$, $(^{207}Pb/^{204}Pb)_t$ and $(^{208}Pb/^{204}Pb)_t$ are Pb isotopic ratios at t = 139 Ma (Yang et al., 2011), calculated by the measured whole-rock U, Th and Pb contents and whole-rock Pb isotopic ratios.

15.60, and $(^{208}Pb/^{204}Pb)_i = 37.92–38.48$ (Table 4), which mostly plot near the field of MORB (Hofmann, 1997) near the intersection of EM-1 and EM-2 (Hofmann, 1997), and are clearly different from those of HIMU (Hofmann, 1997), LCC, UCC (upper continental crust) (Zartman and Haines, 1988) and Dabie adakites derived from the LCC (Huang et al., 2008) (Fig. 9). These are again consistent with isotopic signatures of the LYRB adakitic rocks (Gao et al., 2006; Liu et al., 2010; Wang et al., 2006; Zhou et al., 2007), and Mesozoic mantle derived mafic intrusive rocks from the LYRB (Yan et al., 2008).

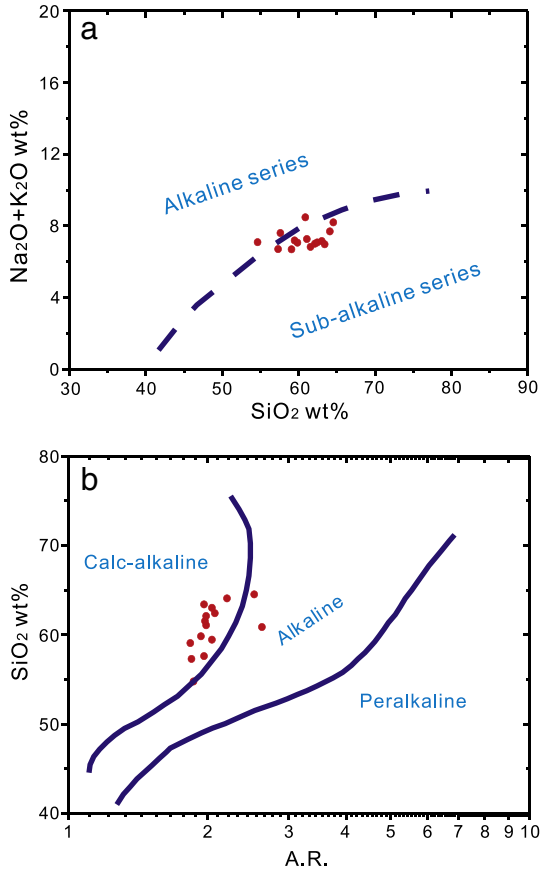

Fig. 4. a) SiO_2–($Na_2O + K_2O$) diagram (Middlemost, 1994). The alkaline and sub-alkaline division is after Irvine and Baragar (1971); b) A.R.–SiO_2 diagram, A.R. = ($Al_2O_3 + CaO + Na_2O + K_2O$)/($Al_2O_3 + CaO - Na_2O - K_2O$). The solid line represents the division among calc-alkaline, alkaline and peralkaline (Geng et al., 2009).

The Sr–Nd–Pb isotopes of the Tongling adakitic rocks can be plausibly interpreted as slab melts contaminated by enriched mantle components without major contributions from the continental crust/sediments.

6. Discussion

6.1. Petrogenesis of dioritic rocks

The Tongling dioritic samples have geochemical features similar to other Mesozoic adakites observed in the LYRB (Gao et al., 2006; Liu et al., 2010; Wang et al., 2003a,b; 2004a,b; 2006; 2007b; G.Q. Xie et al., 2008; Xu et al., 2002; Y.L. Wang et al., 2004). The enrichment of Sr, lack of negative Eu anomalies together with depleted Y and HREE (Fig. 7a) and highly varied $(La/Yb)_N$ (Fig. 6b and Table 2) in the Tongling dioritic rocks (Fig. 7a and b) indicate the existence of garnet rather than plagioclase as a residue in the source (Defant and Kepezhinskas, 2001).

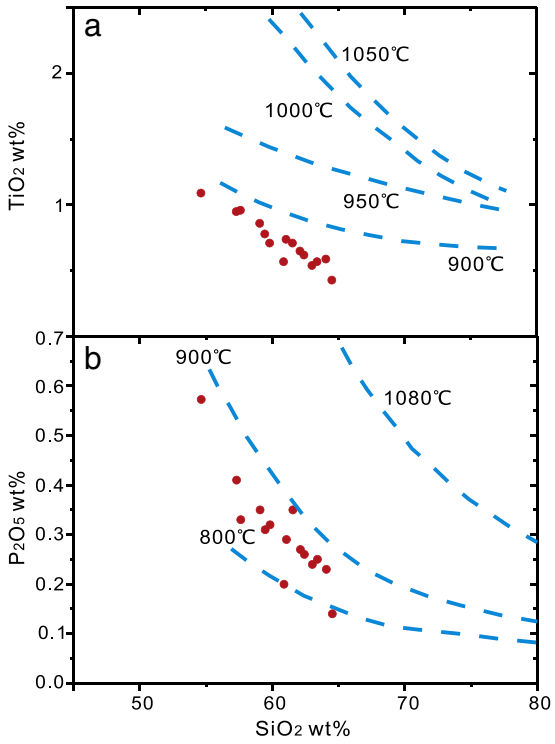

Fig. 5. Harker diagrams for the dioritic rocks from Tongling area. Temperature evaluation based on TiO_2 and P_2O_5 after Harrison and Watson (1984) and Green and Pearson (1986), respectively.

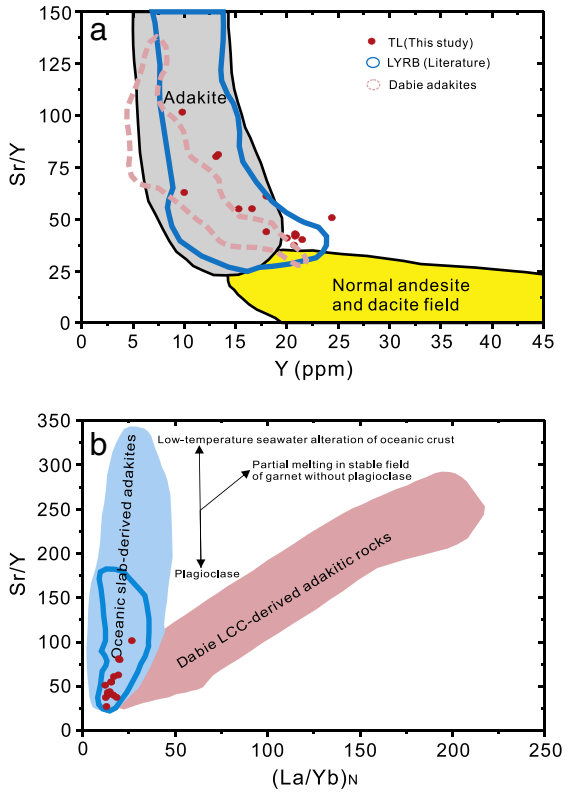

Fig. 6. Plots of Y vs. Sr/Y (a) and Sr/Y vs. $(La/Yb)_N$ (b) for the dioritic rocks in Tongling region, showing adakitic affinity for these rocks, comparable with adakites produced from subducted oceanic slab melting.
Data for slab derived adakites are from Defant and Drummond (1990), Drummond et al. (1996), Stern and Kilian (1996), Aguillón-Robles et al. (2001) and references therein; thickened LCC-derived adakitic rocks from Petford and Atherton (1996), Wang et al. (2007a), Huang et al. (2008), and Zhao and Zhou, 2008; LYRB adakitic rocks from Xu et al. (2002), Wang et al. (2003a and b; 2004a,b; 2006; 2007b), Y.L. Wang et al. (2004), G.Q. Xie et al. (2008), and Liu et al. (2010); and Dabie adakites from Wang et al. (2007a) and Huang et al. (2008).

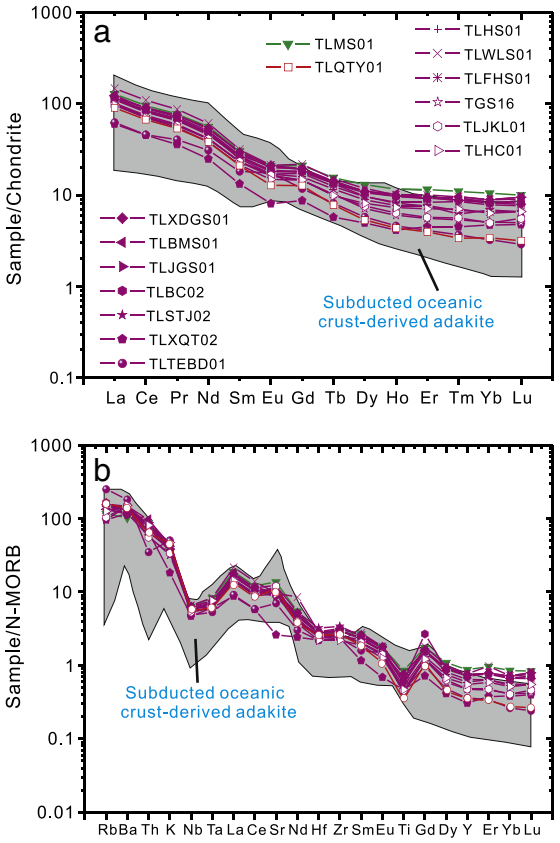

Fig. 7. Rare earth element patterns (a) and spider trace element variation diagrams (b). Chondrite and N-MORB normalizing values after Sun and McDonough (1989). The field of subducted oceanic crust-derived adakites was constructed using data from Defant and Drummond (1990), Kay and Kay (1993), Stern and Kilian (1996), Sajona et al. (2000), Aguillón-Robles et al. (2001), Defant et al. (2002), and Martin et al. (2005).

The strong depletion of both Nb and Ti in the Tongling dioritic rocks (Fig. 7b) suggests that the source has residual rutile (Xiong, 2006). The highly varied and overall subchondritic Nb/Ta may be plausibly interpreted by Nb, Ta fractionation under thermal gradient at the early stage of subduction (Ding et al., 2009; J.L. Liang et al., 2009; Xiao et al., 2006). In general, the P–T conditions of most eclogites are below the dry solidus line. Therefore, dry eclogite without amphibole usually cannot be partially melted. The Tongling adakitic magmas are best explained as having formed through dehydration melting of subducting oceanic crust during the transition from amphibolite to eclogite (e.g., Xiao et al., 2006; Xiong, 2006), a process which readily accounts for their negative Nb, Ta and Ti anomalies, the inconspicuous Eu depletion, positive Sr anomalies and obvious HREE depletion.

The petrogenesis of these adakites in the LYRB has been under debate in the past decade (Hou et al., 2007; Li et al., 2009; Ling et al., 2009, 2011; Liu et al., 2010; Sun et al., 2010, 2011; Wang et al., 2003a,b; 2004a,b; 2006; 2007b; G.Q. Xie et al., 2008; Xu et al., 2002; Zhang et al., 2001). Based on similar whole chemical compositions, but lower initial Nd isotopic compositions relative to adakites from a subducted oceanic slab, some authors proposed that these adakitic rocks had originated from partial melting of the delaminated lower continental crust (LCC) of the Yangtze block, followed by interaction with the mantle peridotites (Wang et al., 2003a,b; 2004a,b; 2006; 2007b; Xu et al., 2002). In contrast, other models such as fractional crystallization of basaltic magmas possibly coupled with crustal contamination (Li et al., 2009; G.Q. Xie et al., 2008), and/or partial melting of subducted oceanic crust (Ling et al., 2009; Liu et al., 2010; Sun et al., 2011), likely during a ridge subduction (Ling et al., 2009, 2011; Sun et al., 2007a, 2010) have also been proposed.

Adakites with different origins display different geochemical characteristics, such as MgO, TiO_2, P_2O_5, Th and U contents, and K_2O/Na_2O, Th/Ce, Th/U, Sr/Y, Sr/La, Ce/Pb and $(La/Yb)_N$ ratios. Samples of

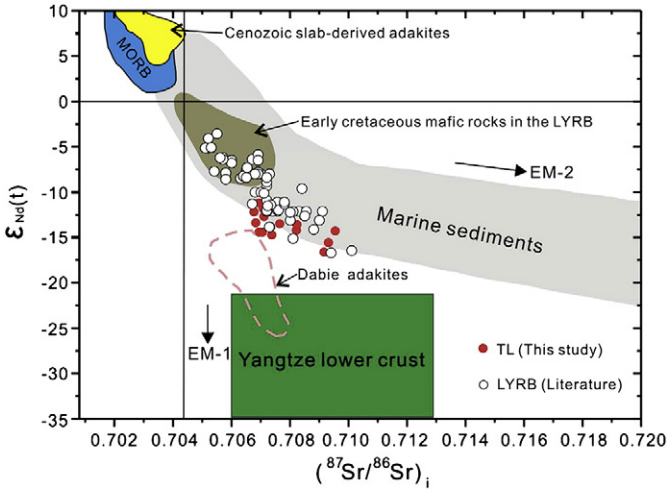

Fig. 8. Nd–Sr isotopic components diagram for the dioritic rocks in the Tongling region. Data source: MORB (Hofmann, 1997) and Marine sediments (Hofmann, 2003); Cenozoic slab-derived adakites (Defant and Kepezhinskas, 2001); Yangtze lower crust (Chen and Jahn, 1998; Xing et al., 1994); Early Cretaceous mafic rocks in the LYRB (Wang et al., 2006; Yan et al., 2008); LYRB adakitic rocks (Wang et al., 2003a and b; 2004 a and b; 2006; 2007b; G.Q. Xie et al., 2008; Liu et al., 2010); and Dabie adakites (Huang et al., 2008; Wang et al., 2007a).

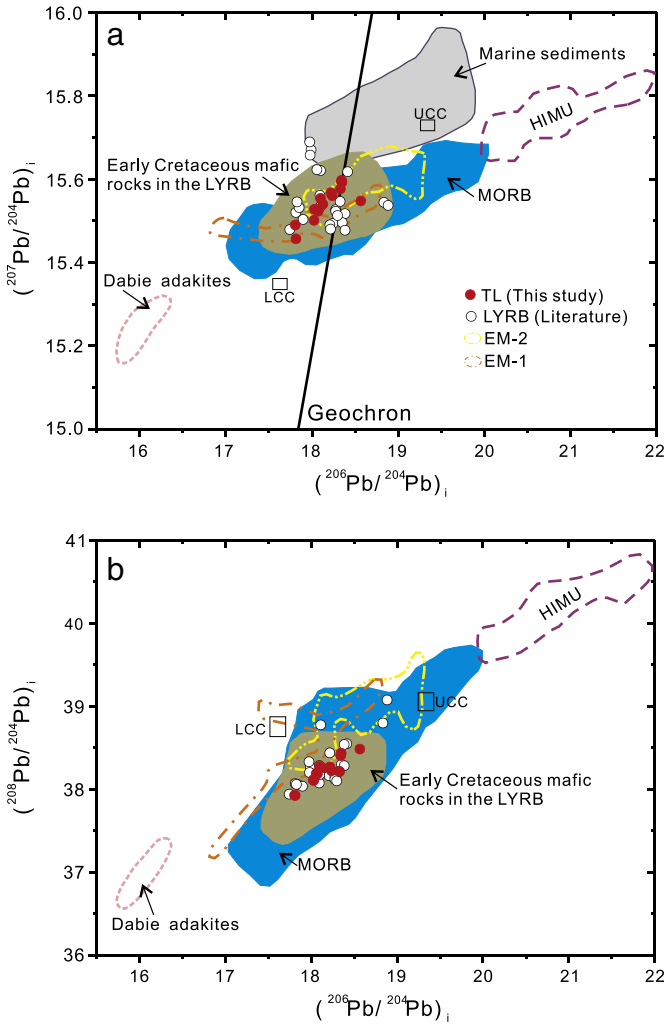

Fig. 9. Initial Pb isotope ratios of the dioritic rocks in the Tongling area. The Tongling dioritic rocks have obviously higher $(^{206}Pb/^{204}Pb)_i$, $(^{207}Pb/^{204}Pb)_i$ and $(^{208}Pb/^{204}Pb)_i$ than Dabie adakites derived from thickened lower crust. The solid line labeled "Geochron" marks the locus of possible primitive mantle values assuming an overall age of the mantle of 4.50 Gyr (Faure, 1986; Galer and Goldstein, 1996). Upper continental crust and LCC mark average compositions of upper and lower continental crust, respectively (Zartman and Haines, 1988).
MORB, HIMU, EM-1 and EM-2 are from Hofmann (1997). Early Cretaceous mafic rocks in the LYRB are after Wang et al. (2006) and Yan et al. (2008). LYRB adakitic rocks are after Gao et al. (2006), Wang et al. (2006), Zhou et al. (2007) and Liu et al. (2010); Dabie adakites are from Huang et al. (2008). Data sources for MORB and Marine sediments are the same as in Fig. 8.

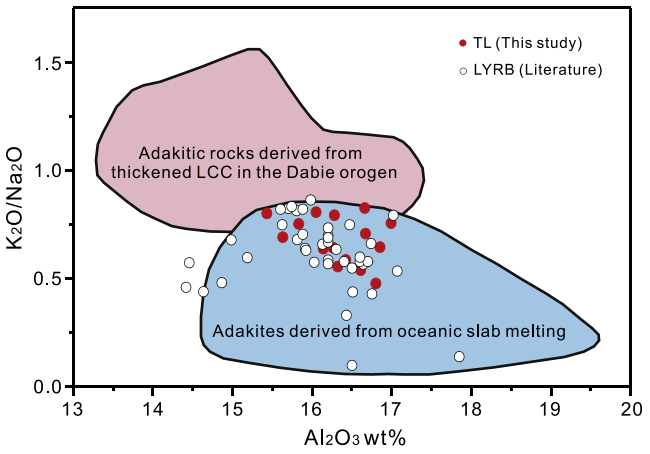

Fig. 10. K_2O/Na_2O versus Al_2O_3 diagram comparing the Tongling dioritic rocks, thickened lower crust-derived adakitic rocks from the Dabie orogen (Huang et al., 2008; Wang et al., 2007a), and oceanic slab-derived adakites (Kamei et al., 2009). Data source of LYRB adakitic rocks is same as in Fig. 9.

Tongling dioritic rocks have Al_2O_3 contents of 15.4 to 17.0 wt.% with an average of 16.3 wt.%, and K_2O/Na_2O ratios ranging from 0.54 to 0.83 with an average of 0.68. These contents generally agree with those of oceanic slab-derived adakites (Fig. 10), and are obviously lower than those of Dabie adakitic rocks derived from the LCC (Huang et al., 2008), showing the presence or absence of amphibole in sources. Amphibole as the primary K-bearing mineral has much higher K_2O than garnet and clinopyroxene in residual phases (e.g., Rapp and Watson, 1995; Sen and Dunn, 1994). The presence of amphibole in the residue can buffer the K concentration in the melt, and thus produce low-K silicious melts. Oceanic adakites with Na-enrichment and K-depletion are products of partial melting of the MORB compositions with amphibole in the residual (Defant and Drummond, 1990; Martin et al., 2005; Rapp and Watson, 1995; Sen and Dunn, 1994). On the other hand, partial melting of dry mafic LCC rocks with an eclogite residual assemblage without amphibole may produce high K melts (Huang and He, 2010; Liu et al., 2010). Therefore, based on the relatively low K content, the Tongling and LYRB adakites likely formed through partial melting of hydrous oceanic crust with residual amphibole during melting.

The MgO contents of the Tongling adakitic rocks vary from 1.05 to 3.50 wt.%, which is typical for adakites formed during slab melting in subduction zones (Defant and Kepezhinskas, 2001). The Mg# is a useful index for discriminating melts of crust origin from those that have interacted with the mantle. Melts from the basaltic lower continental crust are characterized by low Mg# (<0.4) regardless of melting degrees, whereas those with Mg# >0.4 can only be obtained with a mantle component involved (Rapp and Watson, 1995). The dioritic rocks from Tongling and other places in the LYRB have relatively high Mg# (0.35–0.56) (Hou et al., 2007; Liu et al., 2010), indicating the involvement of mantle components.

High Sr/Y and $(La/Yb)_N$ values are two important parameters in the identification of adakites (Defant and Drummond, 1990; Martin et al., 2005; Moyen, 2009). Dioritic rocks of this study have high Sr/Y ratios (37.5–102, average 55.8) and relatively low $(La/Yb)_N$ values (12.2–26.5, average 16.3), which are consistent with those of other LYRB intrusive rocks and Cenozoic adakites from Vizcaino Peninsula in Mexico (Aguillón-Robles et al., 2001). In the Sr/Y versus $(La/Yb)_N$ diagram, all the Tongling samples fall in the field defined by circum-Pacific adakites, which are dramatically different from adakites from the Dabie Mountains (Fig. 6b). The former was derived from slab melting, whereas the latter was formed through lower continental crust melts.

The continental crust has lower Ce/Pb (~4–5; Taylor and McLennan, 1985; Rudnick and Gao, 2003) than the oceanic crust (~24; Sun and McDonough, 1989), and the altered oceanic crust has much higher Sr/La than LCC due to LREE depletion of N-MORB (Sun and McDonough, 1989; Sun et al., 2008) and Sr enrichment by seawater alteration (Liu et al., 2010). The Ce/Pa–Sr/La diagram is useful to discriminate rocks derived from subducted oceanic crust and LCC (Liu et al., 2010). Tongling adakitic rocks have Ce/Pb and Sr/La levels similar to other adakitic rocks from the LYRB, which are higher than those for Dabie adakites, showing an origin from subducted oceanic crust with addition of sediment during melting. The Th/U values (2.51–5.09) from Tongling dioritic rocks of this study are systematically lower and much less variable, which is again consistent with the LYRB adakitic rocks (Ling et al., 2011), falling around the field of N-MORB melts (Sun et al., 2008), but different from mid-continental crust and LCC (Rudnick and Gao, 2003). Thus the Th/U ratios are also evidence for the partial melting of subducted oceanic slab as the origination.

Initial Sr–Nd isotopic compositions at 139 Ma of the Tongling adakitic rocks plot between MORB and enriched mantle (Fig. 8), but are dramatically different from those of the Yangtze lower crust, which are

consistent with those of the LYRB adakites, but different from those of Dabie adakites. The Sr–Nd isotope compositions have been attributed to contamination of slab melts by enriched mantle components or the lower crust (Ling et al., 2009, 2011). Others have also argued that the Sr–Nd isotopic signatures of Tongling and LYRB adakites are typically displaced toward the EM-2 end member, showing the involvement of subducted sediments in magma source (Fig. 8) (Liu et al., 2010).

The Pb isotopic compositions also provide important constraints on the sources of these adakites. The Tongling dioritic rocks are characterized by high radiogenic Pb isotopes with $(^{206}Pb/^{204}Pb)_i = 17.80–18.56$, $(^{207}Pb/^{204}Pb)_i = 15.46–15.60$, and $(^{208}Pb/^{204}Pb)_i = 37.92–38.48$, which mostly plot in the field of MORB, near the intersection EM-1 and EM-2, and are clearly different from those of the upper and lower continental crust, which exclude major contamination from the continental crust (Hofmann, 1997) (Fig. 9). Some samples are plotted in or near the field of marine sediments (Fig. 9a), also implying contribution of subducted sediments. The Tongling and LYRB adakites also both have heavy oxygen isotopic compositions ($\delta^{18}O = +7.55$ to $+11.85$; Chen et al., 1993; Gao et al., 2006; Zhou et al., 2007), supporting sediment involvements. Nevertheless, sediments usually have low Cu concentrations, so that it is not likely to be the dominant component of the Tongling deposits.

Given that eastern China has both EM-1 and EM-2 types of enriched mantle (Zhou et al., 1982; Peng et al., 1986; Xu, 2001), and the transition from EM-1 to EM-2 is located slightly to the north of the Yangtze River close to the Tongling region (Chung, 1999), the enriched Sr–Nd isotopic characteristics of Tongling adakites are best explained by slab melts with assimilation of enriched mantle components. The chemical and isotopic signatures of the Tongling and LYRB adakites strongly support an origin of subducted slab melting with limited contribution from subducted sediments, followed by interaction with the enriched mantle during magma ascending processes. Adakitic magmas formed at ~800–900 °C, which is not hot enough to melt the enriched mantle completely. Instead, adakitic magmas cause small degrees of partial melting of the enriched mantle during its way up, i.e. assimilation. Therefore, the assimilation process can be modeled by mixing of adakitic magmas with basaltic magmas that have Sr–Nd more than 20 times higher than the primitive mantle values (Ling et al., 2009), which correspond to 5% to 10% of partial melting of the enriched mantle components.

Our studies do not support previous models involving partial melting of delaminated or thickened Yangtze lower continental crust (e.g., Hou et al., 2007; Wang et al., 2003a,b, 2007b; Xu et al., 2002; Zhang et al., 2001). In addition to the chemical and isotopic characteristics mentioned above, the LCC usually has lower Cu concentrations (Rudnick and Gao, 2003) under lower oxygen fugacity, which are not favorable for Cu mineralization (Sun et al., 2011, 2012).

6.2. Tectonic setting

The geodynamic setting and tectonic regime of the intensive and widespread Jurassic to Cretaceous magmatism and incidental mineral deposits in the LYRB remain controversial. Some authors have suggested an extensional tectonic setting (e.g., Li et al., 2009; Wang et al., 2007b; G.Q. Xie et al., 2008; Yan et al., 2008), based on the occurrence of Early Cretaceous high-K volcanic rocks and the development of expanding basins. In contrast, adakites have also been attributed to partial melting of thickened or delaminated LCC (Wang et al., 2006; Xu et al., 2002; Zhang et al., 2001), which presumably requires compression. Recent studies suggest that eastern China was an active continental margin from the Jurassic to the Cretaceous, which was closely associated with subduction of the paleo-Pacific plate (Zhou et al., 2006; Li and Li, 2007; Sun et al., 2007a). When the paleo-Pacific plate subduction reached the Yangtze craton, it encountered the mountain root of the Dabie orogen and the North China craton in the north and northwest (e.g. Ernst et al., 2007; Huang and Zhao, 2006). Such a tectonic switch from the Late Jurassic transpressive to the Early Cretaceous extensional regimes in eastern China was considered to be related to the change from the oblique, shallow subduction of the Izanagi Plate to the orthogonal, steep subduction of the Pacific Plate (Zhu et al., 2010). Alternatively, a ridge subduction model, i.e., subduction of a spreading ocean ridge, was proposed for the genesis of the adakitic rocks in the LYRB at the early Cretaceous (Ling et al., 2009, 2011; Sun et al., 2010), based on different drifting directions and rates of the Izanagi plate (Maruyama et al., 1997) and the Pacific Plate (Sun et al., 2007a). The model proposed that the ridge between the two plates was very likely subducted underneath eastern China along the LYRB at ~140 Ma (Ling et al., 2009). These adakitic rocks were derived from partial melting of subducting young, hot oceanic slabs close to the ridge, followed by a slab window and A-type granites (Li et al., 2011, 2011-this issue).

The dioritic rocks in this study are similar to the high-Si adakites and completely different from the low-Si adakites as defined by Martin et al. (2005), supporting the slab melting model. Martin (1998) proposed that formation of these kinds of adakites requires high temperature, which is also consistent with the high formation temperature estimated using conventional geothermometers (Fig. 5a and b).

6.3. Metallogenic significance

Ore deposits in the Tongling and other Lower Yangtze metallogenic belt are closely associated with adakitic igneous rocks (Fig. 1) (Chang et al., 1991; Mao et al., 2006, 2008). In the central belt, deposits are mainly Cu, Au skarn and strata-bound types; at the south and north sides, mineralization is much weaker, whereas the deposits are Cu-polymetallic porphyry type (e.g., Yaojialing deposit of Shatanjiao ore field) (Fig. 1b). The genetic links between adakites and their associated Cu–Au deposits in the LYRB remain a subject of considerable debate. For example, scholars have suggested that Cu–Au mineralization was related to adakite-like rocks generated by partial melting of the lower crust (Hou et al., 2007; Wang et al., 2003b, 2006), most likely derived from the thickened mafic lower crust source, involving various proportions of juvenile mantle components (Hou et al., 2007). In contrast, Ling et al. (2009) proposed that the linear distributions of igneous rocks and ore deposits in the LYRB can best be explained by the subduction of a ridge between the Pacific and Izanagi plates, which is supported by their slab melting origin as suggested by geochemical characteristics (Ling et al., 2011; Liu et al., 2010).

A large number of studies suggested that large-scale Cu (Au) metallogenesis is usually closely associated with convergent margin magmas with high oxygen fugacity (Sillitoe, 1997; Sun et al., 2004; Ulrich et al., 1999), especially in the subducted environments that produce adakitic rocks (Liu et al., 2010; Mungall, 2002; Sun et al., 2010). With similarity to other Cu–Au deposits worldwide (Liang et al., 2006; H.Y. Liang et al., 2009; Mungall, 2002; Sillitoe, 1997; Sun et al., 2004), most ore deposits in the LYRB are associated with adakitic igneous rocks of high oxygen fugacity (Xie et al., 2009).

The high oxygen fugacity of the ore-forming systems in the LYRB was previously attributed to the high water contents or elevated Fe_2O_3 content in adakitic magmas formed through melting of thickened continental crust (Hou et al., 2007; Wang et al., 2006). However, the lower continental crust consists mainly of granulite- or eclogite-facies rocks (Rudnick and Gao, 2003; Weber et al., 2002), which are generally much dryer than subducted oceanic crust. With systematic geochemical investigation, Liu et al. (2010) suggested that the Cu–Au ore deposits in the Lower Yangtze River belt could be not due to the ancient LCC-derived magmas, regardless of having interacted with the mantle or not.

Oxygen fugacity in convergent margin magmas is usually considerably higher than magmas from other geologic settings (Ballhaus, 1993; Brandon and Draper, 1996; Parkinson and Arculus, 1999; Sun et al., 2007b), likely due to subduction-released fluids (Brandon and Draper, 1996; Sun et al., 2007b). High oxygen fugacity can extract additional sulfur in the form of sulfate during partial melting, liberating more chalcophile elements, which are consequently scavenged by magmatic fluids when the oxygen fugacity is reduced (Sun et al., 2004). By contrast,

Cu and Au contents in oceanic crust are generally 60–125 ppm (Sun et al., 2003; estimated average 74 ppm from Hofmann, 1988), much higher than those of the mantle (30 ppm; McDonough and Sun, 1995) and continental crust (27 ppm; Rudnick and Gao, 2003), because Cu and Au are incompatible elements. Therefore, the magmas formed by partial melting of the oceanic crust have systemically high Cu and Au concentrations, and are beneficial to mineralization (Sun et al., 2011).

The LYRB adakites are attributed to partial melting of subducted altered oceanic crust (Liu et al., 2010; Xie et al., 2009), which have high oxygen fugacity (Ballard et al., 2002; Kelley and Cottrell, 2009). Consistently, ore-bearing intermediate intrusive rocks of the Tongling region show high positive Ce anomalies (Xie et al., 2009), suggesting magma formation in an oxidized environment. Therefore, the large scale Cu–Au metallogenesis in the Tongling and LYRB is closely related to partial melting of oceanic slab subduction, whereas adakite can be an important indicator for Cu–Au deposit exploration.

7. Conclusions

The Tongling ore-forming dioritic rocks, which are calc-alkaline, consist mainly of three associations: pyroxene diorite–pyroxene monzodiorite association, quartz diorite–quartz monzodiorite association and granodiorite association. All the rocks have adakite-like major and trace element features, including high Al_2O_3 and Sr contents, high Sr/Y and La/Yb ratios, but low Y and Yb contents.

The Tongling adakitic rocks have an EM2-like Sr–Nd–Pb isotopic signature (high radiogenic Pb isotopes, negative ε_{Nd} values, and high $(^{87}Sr/^{86}Sr)_i$ ratio), and lower Mg# and MgO, K_2O/Na_2O, Th/U ratios, and relatively low $(La/Yb)_N$, but varied high Sr/Y, Sr/La, Ce/Pb, Zr/Nb and Zr/Hf ratios, are distinctively different from magmas from either the thickened or delaminated LCC but similar to oceanic adakites from slab melting.

The Tongling dioritic rocks have a high temperature characteristic, which is consistent with a ridge subduction model, which provide feasible explanation for the distribution of igneous rocks and ore deposits in Tongling and LYRB in the Early Cretaceous ($\sim 140 \pm 5$ Ma). Adakites and large-scale Cu–Au metallogenesis in the Tongling and LYRB was formed by partial melting of young, hot subducting oceanic plates near the ridge.

Acknowledgments

We are grateful to Professor Eby for superb editorial handling and two anonymous referees for constructive comments, which are helpful for us to improve the manuscript. This study is supported by the Knowledge Innovation Project of Chinese Academy of Sciences (KZCX1-YW-15-3), the National Natural Science Foundation of China (41173057, 41090372, and 40921002), Research Fund for Doctoral Programs of Higher Education of China (No. 20100111120012), the Excellence Youth Science and Technology Foundation (No. 08040106907), and the Doctorship Foundation from Hefei University of Technology (GDBJ2008-041). Prof. Yinfo Chang is highly appreciated for his constructive suggestions.

References

Aguillón-Robles, A., Calmus, T., Benoit, M., Bellon, H., Maury, R.O., Cotton, J., Bourgois, J., Michaud, F., 2001. Late Miocene adakites and Nb-enriched basalts from Vizcaino Peninsula, Mexico: indicators of East Pacific Rise subduction below Southern Baja California. Geology 29, 531–534.

Ballard, J.R., Palin, J.M., Campbell, I.H., 2002. Oxidized magmas associated with porphyry copper deposits in northern Chile: inferences based on Ce (IV)/Ce (III) in zircon. Contributions to Mineralogy and Petrology 144, 347–364.

Ballhaus, C., 1993. Redox states of lithospheric and asthenospheric upper mantle. Contributions to Mineralogy and Petrology 114, 331–348.

Brandon, A.D., Draper, D.S., 1996. Constraints on the origin of the oxidation state of mantle overlying subduction zones: an example from Simcoe, Washington, USA. Geochimica et Cosmochimica Acta 60, 1739–1749.

Chang, Y.F., Liu, X.P., Wu, Y.C., 1991. The Copper–iron Belt of the Middle and Lower Reaches of the Changjiang River. Geological Publishing House, Beijing. (379 pp.).

Chen, J.F., Jahn, B.M., 1998. Crustal evolution of Southeastern China: Nb and Sr isotopic evidence. Tectonophysics 284, 101–133.

Chen, J.F., Zhou, T.X., Li, X.M., Foland, K.A., Huang, C.Y., Lu, W., 1993. Sr and Nd isotopic constraints on source regions of the intermediate and acidic intrusions from southern Anhui Province. Geochimica (3), 26l–268l (in Chinese with English abstract).

Chung, S.L., 1999. Trace element and isotope characteristics of Cenozoic basalts around the Tanlu fault with implication for the eastern plate boundary between north and south China. Journal of Geology 107, 301–312.

Defant, M.J., Drummond, M.S., 1990. Derivation of some modern arc magmas by melting of young subducted lithosphere. Nature 347, 662–665.

Defant, M.J., Kepezhinskas, P., 2001. Evidence suggests slab melting in arc magmas. EOS (Transactions, American Geophysical Union) 82, 65–69.

Defant, M.J., Xu, J.F., Kepezhinskas, P., Wang, Q., Zhang, Q., Xiao, L., 2002. Adakites: some variations on a theme. Acta Petrologica Sinica 18, 129–142.

Ding, X., Lundstrom, C., Huang, F., Li, J., Zhang, Z.M., Sun, X.M., Liang, J.L., Sun, W.D., 2009. Natural and experimental constraints on formation of the continental crust based on niobium–tantalum fractionation. International Geology Review 51, 473–501.

Drummond, M.S., Defant, M.J., Kepezhinskas, P.K., 1996. Petrogenesis of slab-derived trondhjemite–tonalite–dacite/adakite magmas. 3rd Hutton Symposium on the Origin of Granites and Related Rocks, College Pk, Md, pp. 205–215.

Ernst, W.G., Tsujimori, T., Zhang, R., Liou, J.G., 2007. Permo-Triassic collision, subduction-zone metamorphism, and tectonic exhumation along the East Asian continental margin. Annual Review of Earth and Planetary Sciences 35, 73–110.

Faure, G., 1986. Principles of Isotope Geology. Wiley, New York, pp. 1–589.

Foland, K.A., Allen, J.C., 1991. Magma sources for Mesozoic anorogenic granites of the White Mountain magma series, New England, USA. Contributions to Mineralogy and Petrology 109, 195–211.

Galer, S.J.G., Goldstein, S.L., 1996. In Earth Processes: Reading the Isotopic Code. In: Basu, A., Hart, S.R. (Eds.), Am. Geophys. Union, Washington DC, pp. 75–98.

Gao, G., Xu, Z.W., Yang, X.N., Wang, Y.J., Zhang, J., Jiang, S.Y., Ling, H.F., 2006. Petrogenesis of the Baimangshan pyroxene diorite intrusion in Tongling Area, Anhui Province: constraints from Sr–Nd–Pb–O isotope. Journal of Nanjing University (Natural Sciences) 42 (3), 269–279 (in Chinese with English abstract).

Geng, H.Y., Sun, M., Yuan, C., Xiao, W.J., Xian, W.S., Zhao, G.C., Zhang, L.F., Wong, K., Wu, F.Y., 2009. Geochemical, Sr–Nd and zircon U–Pb–Hf isotopic studies of Late Carboniferous magmatism in the West Junggar, Xinjiang: implications for ridge subduction. Chemical Geology 266, 364–389.

Green, T.H., Pearson, N.J., 1986. Ti-rich accessory phase saturation in hydrous mafic–felsic compositions at high P, T. Chemical Geology 54, 185–201.

Gu, L.X., Fu, S.G., 1999. Fault-induced depressing, volcanism and massive sulphide formation of the Lower Yangtze region at the Weinian stage: a reply. Geological Journal of China Universities 5, 228–231 (in Chinese with English abstract).

Guo, W.M., Lu, J.J., Zhang, R.Q., Xu, Z.W., 2010. Ore textures and genetic significance of pyrrhotite from Dongguashan ore deposit in Tongl ing area, Anhui Province. Mineral Deposits 29 (3), 405–414 (in Chinese with English Abstract).

Harrison, T.M., Watson, E.B., 1984. The behavior of apatite during crustal anatexis-equilibrium and kinetic considerations. Geochimica et Cosmochimica Acta 48, 1467–1477.

Hofmann, A.W., 1988. Chemical differentiation of the Earth: the relationship between mantle, oceanic crust and continental crust. Earth and Planetary Science Letters 90, 297–314.

Hofmann, A.W., 1997. Mantle geochemistry: the message from oceanic volcanism. Nature 385, 219–229.

Hofmann, A.W., 2003. Sampling mantle heterogeneity through oceanic basalts: isotopes and trace elements. In: Carlson, R.W. (Ed.), The Mantle and Core. Treatise on Geochemistry. Elsevier-Pergamon, Oxford (61–101 pp.).

Hou, Z.Q., Pan, X.F., Yang, Z.M., Qu, X.M., 2007. Porphyry Cu–(Mo–Au) deposits not related to oceanic-slab subduction: examples from Chinese porphyry deposits in continental settings. Geoscience 21, 332–351 (in Chinese with English abstract).

Huang, F., He, Y.S., 2010. Partial melting of dry mafic lower continental crust: constraints on formation of C-type adakites. Chinese Science Bulletin 55, 2428–2439.

Huang, J.L., Zhao, D.P., 2006. High-resolution mantle tomography of China and surrounding regions. Journal of Geophysical Research 111, B9305–B9325.

Huang, F., Li, S.G., Dong, F., He, Y.S., Chen, F.K., 2008. High-Mg adakitic rocks in the Dabie orogen, central China: implications for foundering mechanism of lower continental crust. Chemical Geology 255, 1–13.

Irvine, T.N., Baragar, W.R.A., 1971. Guide to chemical classification of common volcanic rocks. Canadian Journal of Earth Sciences 8, 523–548.

Kamei, A., Miyake, Y., Owada, M., Kimura, J.I., 2009. A pseudo adakite derived from partial melting of tonalitic to granodioritic crust, Kyushu, southwest Japan arc. Lithos 112, 615–625.

Kay, R.W., Kay, S.M., 1993. Delamination and delamination magmatism. Tectonophysics 219, 177–189.

Kelley, K.A., Cottrell, E., 2009. Water and the oxidation state of subduction zone magmas. Science 325, 605–607.

Li, Z.X., Li, X.H., 2007. Formation of the 1300-km-wide intracontinental orogen and postorogenic magmatic province in Mesozoic South China: A flat-slab subduction model. Geology 35, 179–182.

Li, S.G., Xiao, Y.L., Liu, D.L., Chen, Y.Z., Ge, N.J., Zhang, Z.Q., Sun, S.S., Cong, B.L., Zhang, R.Y., Stanley, R.H., Wang, S.S., 1993. Collision of the North China and Yangtze blocks and formation of coesite-bearing eclogites, timing and processes. Chemical Geology 109, 89–111.

Li, J.W., Zhao, X.F., Zhou, M.F., Ma, C.Q., Sergio de Souza, Z., Vasconcelos, P., 2009. Late Mesozoic magmatism from Daye region, eastern China: U–Pb ages, petrogenesis, and geodynamic implications. Contributions to Mineralogy and Petrology 157, 383–409.

Li, H., Zhang, H., Ling, M.X., Wang, F.Y., Ding, X., Zhou, J.B., Yang, X.Y., Tu, X.L., Sun, W.D., 2011. Geochemical and zircon U–Pb study of the Huangmeijian A-type granite: implications for geological evolution of the Lower Yangtze River belt. International Geology Review 53 (5–6), 499–525.

Li, H., Ling, M.X., Li, C.Y., Zhang, H., Ding, X., Yang, X.Y., Fan, W.M., Li, Y.L., Sun, W.D., 2011. A-type granite belts of two chemical subgroups in central eastern China: indication of ridge subduction. Lithos 150, 26–36 (this issue).

Liang, H.Y., Campbell, I.H., Allen, C., Sun, W.D., Liu, C.Q., Yu, H.X., Xie, Y.W., Zhang, Y.Q., 2006. Zircon Ce^{4+}/Ce^{3+} ratios and ages for Yulong ore-bearing porphyries in eastern Tibet. Mineralium Deposita 41, 152–159.

Liang, H.Y., Sun, W.D., Su, W.C., Zartman, R.E., 2009a. Porphyry copper–gold mineralization at Yulong, China, promoted by decreasing redox potential during magnetite alteration. Economic Geology 104, 587–596.

Liang, J.L., Ding, X., Sun, X.M., Zhang, Z.M., Zhang, H., Sun, W.D., 2009b. Nb/Ta fractionation observed in eclogites from the Chinese Continental Scientific Drilling Project. Chemical Geology 268, 27–40.

Ling, M.X., Wang, F.Y., Ding, X., Hu, Y.H., Zhou, J.B., Zartman, R.E., Yang, X.Y., Sun, W.D., 2009. Cretaceous ridge subduction along the Lower Yangtze River Belt, eastern China. Economic Geology 104, 303–321.

Ling, M.X., Wang, F.Y., Ding, X., Zhou, J.B., Sun, W.D., 2011. Different origins of adakites from the Dabie Mountains and the Lower Yangtze River belt in eastern China: geochemical constraints. International Geology Review 53 (5–6), 727–740.

Liu, S.A., Li, S.G., He, Y.S., Huang, F., 2010. Geochemical contrasts between early Cretaceous ore-bearing and ore-barren high-Mg adakites in central-eastern China: implications for petrogenesis and Cu–Au mineralization. Geochimica et Cosmochimica Acta 74, 7160–7178.

Lu, J.J., Guo, W.M., Chen, W.F., Jiang, S.Y., Li, J., Yan, X.R., Xu, Z.W., 2008. A metallogenic model for the Dongguashan Cu–Au deposit of Tongling, Anhui Province. Acta Petrologica Sinica 24 (8), 1857–1864.

Mao, J.W., Wang, Y.T., Lehmann, B., Yu, J.J., Du, A.D., Mei, Y.X., Li, Y.F., Zang, W.S., Stein, H.J., Zhou, T.F., 2006. Molybdenite Re–Os and albite $^{40}Ar/^{39}Ar$ dating of Cu–Au–Mo and magnetite porphyry systems in the Yangtze River valley and metallogenic implications. Ore Geology Reviews 29, 307–324.

Mao, J.W., Xie, G.Q., Bierlein, F., Qu, W.J., Du, A.D., Ye, H.S., Pirajno, F., Li, H.M., Guo, B.J., Li, Y.F., Yang, Z.Q., 2008. Tectonic implications from Re–Os dating of Mesozoic molybdenum deposits in the East Qinling–Dabie orogenic belt. Geochimica et Cosmochimica Acta 72, 4607–4626.

Martin, H., 1998. Adakitic magmas: modern analogues of Archaean granitoids. Bahia, Brazil, International Symposium on Granites and Associated Mineralisations (ISGAM), pp. 411–429.

Martin, H., 1999. Adakitic magmas: modern analogues of Archaean granitoids. Lithos 46, 411–429.

Martin, H., Smithies, R.H., Rapp, R., Moyen, J.F., Champion, D., 2005. An overview of adakite, tonalite–trondhjemite–granodiorite (TTG), and sanukitoid: relationships and some implications for crustal evolution. Lithos 79, 1–24.

Maruyama, S., Isozaki, Y., Kimura, G., Terabayashi, M., 1997. Paleogeographic maps of the Japanese Islands: Plate tectonic synthesis from 750 Ma to the present. Island Arc 6, 121–142.

McDonough, W.F., Sun, S.S., 1995. The composition of the Earth. Chemical Geology 120, 223–253.

Middlemost, E.A.K., 1994. Naming materials in the magma igneous rock system. Earth-Science Reviews 37, 215–224.

Moyen, J.F., 2009. High Sr/Y and La/Yb ratios: the meaning of the 'adakitic signature'. Lithos 112, 556–574.

Mungall, J.E., 2002. Roasting the mantle: Slab melting and the genesis of major Au and Au-rich Cu deposits. Geology 30, 915–918.

Pan, Y.M., Dong, P., 1999. The Lower Changjiang (Yangzi/Yangtze River) metallogenic belt, east central China: intrusion- and wall rock-hosted Cu–Fe–Au, Mo, Zn, Pb, Ag deposits. Ore Geology Reviews 15, 177–242.

Parkinson, I.J., Arculus, R.J., 1999. The redox state of subduction zones: insights from arc-peridotites. Chemical Geology 160, 409–423.

Peng, Z.C., Zartman, R.E., Futa, K., Chen, D.G., 1986. Pb-Isotopic, Sr-Isotopic and Nd-Isotopic Systematics and Chemical Characteristics of Cenozoic Basalts, Eastern China. Chemical Geology 59 (1), 3–33.

Petford, N., Atherton, M., 1996. Na-rich partial melts from newly underplated basaltic crust: the Cordillera Blanca Batholith, Peru. Journal of Petrology 37, 1491–1521.

Rapp, R.P., Watson, E.B., 1995. Dehydration melting of metabasalt at 8–32-kbar: implications for continental growth and crust–mantle recycling. Journal of Petrology 36, 891–931.

Rudnick, R.L., Gao, S., 2003. Composition of the continental crust. In: Holland, H.D., Turekian, K.K. (Eds.), Treatise on Geochemistry. Elsevier, Oxford, UK.

Sajona, F.G., Maury, R.C., Pubellier, M., Leterrier, J., Bellon, H., Cotten, J., 2000. Magmatic source enrichment by slab-derived melts in a young post-collision setting, central Mindanao (Philippines). Lithos 54, 173–206.

Sen, C., Dunn, T., 1994. Dehydration melting of a basaltic composition amphibolite at 1.5 and 2.0 GPa: implications for the origin of adakites. Contributions to Mineralogy and Petrology 117, 394–409.

Sillitoe, R.H., 1997. Characteristics and controls of the largest porphyry Cu–Au and epithermal Au deposits in the circum-Pacific region. Australian Journal of Earth Sciences 44, 373–388.

Stern, C.R., Kilian, R., 1996. Role of the subducted slab, mantle wedge and continental crust in the generation of adakites from the Andean Austral volcanic zone. Contributions to Mineralogy and Petrology 123, 263–281.

Sun, S.S., McDonough, W.F., 1989. Chemical and isotopic systematics of oceanic basalts: implication for mantle composition and processes. Geological Society Special Publication 42, 313–345.

Sun, W.D., Li, S.G., Sun, Y., Zhang, G.W., Li, Q.L., 2002. Mid-paleozoic collision in the north Qinling: Sm–Nd, Rb–Sr and $^{40}Ar/^{39}Ar$ ages and their tectonic implications. Journal of Asian Earth Sciences 21, 69–76.

Sun, W.D., Xie, Z., Chen, J.-F., Zhang, X., Chai, Z.F., Du, A.D., Zhao, J.S., Zhang, C.H., Zhou, T.F., 2003. Os–Os dating of copper and molybdenum deposits along the middle and lower reaches of Yangtze River, China. Economic Geology 98, 175–180.

Sun, W.D., Arculus, R.J., Kamenetsky, V.S., Binns, R.A., 2004. Release of gold-bearing fluids in convergent margin magmas prompted by magnetite crystallization. Nature 431, 976–978.

Sun, W.D., Ding, X., Hu, Y.H., Li, X.H., 2007a. The golden transformation of the Cretaceous plate subduction in the west Pacific. Earth and Planetary Science Letters 262, 533–542.

Sun, X.M., Tang, Q., Sun, W.D., Xu, L., Zhai, W., Liang, J.L., Liang, Y.H., Shen, K., Zhang, Z.M., Zhou, B., Wang, F.Y., 2007b. Monazite, iron oxide and barite exsolutions in apatite aggregates from CCSD drillhole eclogites and their geological implications. Geochimica et Cosmochimica Acta 71, 2896–2905.

Sun, W.D., Hu, Y.H., Kamenetsky, V.S., Eggins, S.M., Chen, M., Arculus, R.J., 2008. Constancy of Nb/U in the mantle revisited. Geochimica et Cosmochimica Acta 72, 3542–3549.

Sun, W.D., Ling, M.X., Yang, X.Y., Fan, W.M., Ding, X., Liang, H.Y., 2010. Ridge subduction and porphyry copper gold mineralization. Science in China Series D Earth Sciences 53 (4), 475–484.

Sun, W.D., Ling, M.X., Ding, X., Chung, S.L., Zhou, J.B., Yang, X.Y., Fan, W.M., 2011. The association between adakites and Cu–Au ore deposits. International Geology Review 53 (5–6), 691–703.

Sun, W.D., Ling, M.X., Chung, S.L., Ding, X., Yang, X.Y., Liang, H.Y., Fan, W.M., Goldfarb, R., Yin, Q.Z., 2012. Geochemical constraints on adakites of different origins and copper mineralization. Journal of Geology 120 (1), 105–120.

Taylor, S.R., McLennan, S.M., 1985. The Continental Crust: Its Composition and Evolution. Blackwell Scientific Publications, Oxford. 100 pp.

Ulrich, T., Guether, D., Heinrich, C.A., 1999. Gold concentrations of magmatic brines and the metal budget of porphyry copper deposits. Nature 399, 676–679.

Wang, Q., Zhao, Z.H., Xu, J.F., Li, X.H., Xiong, X.L., Bao, Z.W., 2003a. Petrogenesis of the Mesozoic intrusive rocks in the Tongling area, Anhui Province, China and their constraint on geodynamic process. Science in China Series D Earth Sciences 46, 801–815.

Wang, Q., Zhao, Z.H., Xu, J.F., Li, X.H., Xiong, X.L., Bao, Z.W., Liu, Y.M., 2003b. Petrogenesis and metallogenesis of the Yanshanian adakite-like rocks in the Eastern Yangtze block. Science in China Series D Earth Sciences 46 (Suppl.), 164–176.

Wang, Y.L., Wang, Y., Zhang, Q., Jia, X.Q., Han, S., 2004a. The geochemical characteristics of Mesozoic intermediate-acid intrusives of the Tongling area and its metallogenesis-geodynamic implications. Acta Petrologica Sinica 20, 325–338.

Wang, Q., Xu, J.F., Zhao, Z.H., Bao, Z.W., Xu, W., Xiong, X.L., 2004b. Cretaceous high-potassium intrusive rocks in the Yueshan–Hongzhen area of east China: adakites in an extensional tectonic regime within a continent. Geochemical Journal 38, 417–434.

Wang, Q., Zhao, Z.H., Bao, Z.W., Xu, J.F., Liu, W., Li, C.F., Bai, Z.H., Xiong, X.L., 2004c. Geochemistry and petrogenesis of the Tongshankou and Yinzu adakitic intrusive rocks and the associated porphyry copper–molybdenum mineralization in southeast Hubei, east China. Resource Geology 54, 137–152.

Wang, Q., Wyman, D.A., Xu, J.F., Zhao, Z.H., Jian, P., Xiong, X.L., Bao, Z.W., Li, C.F., Bai, Z.H., 2006. Petrogenesis of Cretaceous adakitic and shoshonitic igneous rocks in the Luzong area, Anhui Province (eastern China): implications for geodynamics and Cu–Au mineralization. Lithos 89, 424–446.

Wang, Q., Wyman, D.A., Xu, J.F., Jian, P., Zhao, Z.H., Li, C., Xu, W., Ma, J., He, B., 2007a. Early Cretaceous adakitic granites in the Northern Dabie complex, central China: implications for partial melting and delamination of thickened lower crust. Geochimica et Cosmochimica Acta 71, 2609–2636.

Wang, Q., Wyman, D.A., Xu, J.F., Zhao, Z.H., Jian, P., Zi, F., 2007b. Partial melting of thickened or delaminated lower crust in the middle of Eastern China: implications for Cu–Au mineralization. Journal of Geology 115, 149–161.

Weber, M.B.I., Tarney, J., Kempton, P.D., Kent, R.W., 2002. Crustal make-up of the northern Andes: Evidence based on deep crustal xenolith suites, Mercaderes, SW Colombia. Tectonophysics 345, 49–82.

Wu, G.G., Zhang, D., Di, Y.J., Zang, W.Q., Zhang, X.X., Song, B., Zhang, Z.Y., 2008. SHRIMP zircon U–Pb dating of the intrusives in the Tongling metallogenic cluster and its dynamic setting. Science in China Series D Earth Sciences 51 (7), 911–928.

Xiao, Y.L., Sun, W.D., Hoefs, J., Simon, K., Zhang, Z.M., Li, S.G., Hofmann, A.W., 2006. Making continental crust through slab melting: constrains from niobium–tantalum fractionation in UHP metamorphic rutile. Geochimica et Cosmochimica Acta 70, 4770–4782.

Xie, G.Q., Mao, J.W., Li, R.L., Bierlein, F.P., 2008a. Geochemistry and Nd–Sr isotopic studies of Late Mesozoic granitoids in the southeastern Hubei Province, Middle–Lower Yangtze River belt, Eastern China: petrogenesis and tectonic setting. Lithos 104, 216–230.

Xie, J.C., Yang, X.Y., Du, J.G., Sun, W.D., 2008b. Zircon U–Pb geochronology of the Mesozoic intrusive rocks in the Tongling region: implications for copper–gold mineralization. Acta Petrologica Sinica 24 (8), 1782–1800.

Xie, J.C., Yang, X.Y., Sun, W.D., Du, J.G., Xu, W., Wu, L.B., Wang, K.Y., Du, X.W., 2009. Geochronological and geochemical constraints on formation of the Tongling metal deposits, middle Yangtze metallogenic belt, east-central China. International Geology Review 51, 388–421.

Xing, F.M., Xu, X., 1996. High-potassisum calc-alkaline intrusive rocks in Tongling area, Anhui Province. Geochimica 25, 29–38.

Xing, F.M., Xu, X., Li, Z.C., 1994. Discovery of the Early Proterozoic basement in the Middle–Lower Reaches of Yangtze River and its significance. Chinese Science Bulletin 39, 136–139.

Xiong, X.L., 2006. Trace element evidence for growth of early continental crust by melting of rutile-bearing hydrous eclogite. Geology 34, 945–948.
Xu, Y.G., 2001. Thermo-tectonic destruction of the Archaean lithospheric keel beneath the Sino-Korean Craton in China: Evidence, timing and mechanism. Physics and Chemistry of the Earth Part A—Solid Earth and Geodesy 26, 747–757.
Xu, G., Zhou, J., 2001. The Xinqiao Cu–S–Fe–Au deposit in the Tongling mineral district, China: synorogenic remobilization of a stratiform sulfide deposit. Ore Geology Reviews 18, 77–94.
Xu, J.F., Shinjo, R., Defant, M.J., Wang, Q., Rapp, R.P., 2002. Origin of Mesozoic adakitic intrusive rocks in the Ningzhen area of east China: partial melting of delaminated lower continental crust. Geology 30, 1111–1114.
Xu, X.S., Fan, Q.C., O'Reilly, S.Y., Jiang, S.Y., Griffin, W.L., Wang, R.C., Qiu, J.S., 2004. U–Pb dating of zircons from quartz diorite and its enclaves at Tongguanshan in Anhui and its petrogenetic implication. Chinese Science Bulletin 49, 2073–2082.
Yan, J., Chen, J.F., Xu, X.S., 2008. Geochemistry of Cretaceous mafic rocks from the Lower Yangtze region, eastern China: characteristics and evolution of the lithospheric mantle. Journal of Asian Earth Sciences 33, 177–193.
Yang, X.Y., Lee, I.S., 2011. Review of the stable isotope geochemistry of Mesozoic igneous rocks and Cu–Au deposits along the middle–lower Yangtze Metallogenic Belt, China. International Geology Review 53 (5–6), 741–757.
Yang, X.N., Xu, Z.W., Lu, X.C., Jiang, S.Y., Ling, H.F., Liu, L.G., Chen, D.Y., 2011. Porphyry and skarn Au–Cu deposits in the Shizishan orefield, Tongling, East China: U–Pb dating and in-situ Hf isotope analysis of zircons and petrogenesis of associated granitoids. Ore Geology Reviews 43 (1), 182–193.
Zartman, R.E., Haines, S.M., 1988. The plumbotectonic model for Pb isotopic systematics among major terrestrial reservoirs — a case for bi-directional transport. Geochimica et Cosmochimica Acta 52, 1327–1339.
Zhai, Y.S., Xiong, Y.L., Yao, S.Z., Lin, X.D., 1996. Metallogeny of copper and iron deposits in the Eastern Yangtze Craton, east-central China. Ore Geology Reviews 11, 229–248.
Zhang, Q., Wang, Y., Qian, Q., 2001. The characteristics and tectonic–metallogenic significances of the adakites in Mesozoic period from eastern China. Acta Petrologica Sinica 17, 236–244 (in Chinese with English abstract).
Zhao, J.H., Zhou, M.F., 2008. Neoproterozoic adakitic plutons in the northern margin of the Yangtze Block, China: partial melting of a thickened lower crust and implications for secular crustal evolution. Lithos 104, 231–248.
Zhou, X., Armstrong, R.L., 1982. Cenozoic volcanic-rocks of eastern China-Secular and geographic trends in chemistry and strontium Isotopic composition. Earth and Planetary Science Letters 58 (3), 301–329.
Zhou, X.M., Sun, T., Shen, W.Z., Shu, L.S., Niu, Y.L., 2006. Petrogenesis of Mesozoic granitoids and volcanic rocks in South China: a response to tectonic evolution. Episodes 29, 26–33.
Zhou, T.F., Yuan, F., Yue, S.C., Liu, X.D., Zhang, X., Fan, Y., 2007. Geochemistry and evolution of ore-forming fluids of the Yueshan Cu–Au skarn- and vein-type deposits, Anhui Province, South China. Ore Geology Reviews 31, 279–303.
Zhou, T.F., Zhang, L.J., Yuan, F., Fan, Y., Cooke, D.R., 2010. LA-ICP-MS in situ trace element analysis of pyrite from the Xinqiao Cu–Au–S deposit in Tongling, Anhui, and its constraints on the ore genesis. Earth Science Frontiers 17 (2), 306–319 (in Chinese with English Abstract).
Zhu, G., Niu, M., Xie, C., Wan, Y., 2010. Sinistral to normal faulting along the Tan–Lu Fault Zone: evidence for geodynamic switching of the East China continental margin. Journal of Geology 118, 277–293.